OPTIMIZING ZWITTERIONIC COATINGS FOR ANTI-FOGGING, ABRASION RESISTANT HIGH-PERFORMANCE EYEWEAR

by

MADISON SMITH

((Under the Direction of Jason Locklin)

ABSTRACT

This work aims to deepen the understanding of zwitterionic copolymer coatings and the necessary optimization to achieve anti-fog and abrasion resistant properties in high performance eyewear. A zwitterionic copolymer, 2-methacryloyloxyethyl phosphorylcholine-co-butyl methacrylate-co-benzophenone (BPMPC), was photochemically grafted to available hydrogens via the benzophenone (BP) moiety to produce a robust crosslinked network. It was established that monomer purity in solution was imperative for abrasion resistance, and BPMPC functional coatings are limited by the type of substrate they can photocrosslink to. Substrates containing C-H bonds that undergo BP hydrogen abstraction at slower rates than that of the polymer chain, will not create robustly crosslinked networks resulting in loss of abrasion resistant. Finally, it was determined that kinetics of crosslinking are affected by wavelength of irradiation and that photobleaching and oxidation of benzophenone occurred in an oxygenated atmosphere. The findings from this research have led to a greater understanding of the BPMPC polymer system.

INDEX WORDS: ZWITTERIONIC, ANTI-FOG, ABRASION-RESISTANT, BENZOPHENONE, PHOTOCROSSLINK, KINETICS, OXIDATION

OPTIMIZING ZWITTERIONIC COATINGS FOR ANTI-FOGGING, ABRASION RESISTANT HIGH-PERFORMANCE EYEWEAR

by

MADISON SMITH

BS, Bradley University, 2017

A Thesis Submitted to the Graduate Faculty of The University of Georgia in Partial Fulfillment of the Requirements for the Degree

MASTER OF SCIENCE

ATHENS, GEORGIA

2020

OPTIMIZING ZWITTERIONIC COATINGS FOR ANTI-FOGGING, ABRASION RESISTANT HIGH-PERFORMANCE EYEWEAR

by

MADISON SMITH

Major Professor:	Jason Locklin
Committee:	Sergiy Minko
	Hitesh Handa

Electronic Version Approved:

Ron Walcott
Interim Dean of the Graduate School
The University of Georgia
August 2020

DEDICATION

To my family, without your unconditional love and support this would not have been possible. You were there to help me become my best, and never judged me when I didn't always know what my best was or how I was going to get there. Life has many challenges, and things don't always work out as planned, but along the way you have always been there as I have grown into who I am today. For my mom, who taught me grace and love, and was always proud of me. For my father, who challenged me every day to work hard and to walk with conviction. For my sisters, who were the best role models I could have ever asked for, I am so proud to be their sister. I am forever grateful for every opportunity you have given me, and I know I have a lot to be thankful for.

ACKNOWLEDGEMENTS

I want to thank my family, whose support and love got me through my studies. I could not have accomplished this without you. Thank you to my parents, who have given me the world; you encouraged and comforted me when I needed it the most. Thank you for Zeta, who became my needed oasis and friend. It was you who made me realize that this journey made me stronger, and let me know that I could overcome any difficulties and challenges that I might face.

Next, I want to thank Dr. Jason Locklin. You taught me to not give up when everything is going wrong; you taught me to stand up for myself and be confident; you taught me to aim high in my goals, and helped picked me back up when I didn't always meet them. Thank you for the time and effort that you put in to making me better, I truly hope that one day I will be as dedicated, intelligent, aspiring, and confident as you are. Thank you for letting me choose my own path and understanding why I had to do it. I promise that one day I will show you what I have accomplished on my next journey, and I hope that it makes you proud. To my committee members, Dr. Minko and Dr. Handa, thank you for your time, teachings, and advice in my studies and project. Thank you also for being patient and understanding when the world throws us a challenge.

Lastly, I want to thank all of my collaborators and lab mates. Thank you to Melissa Roth and Michelle Markey, for their collaboration and funding at NSRDEC. Thank you for your understanding and encouragement when things didn't always go as planned. I want to thank Yutian for letting me see what a truly great scientist looks like; to Tim for all of the laughs, you always brightened my day; to Scott and DeMichael for all of your fun antics in lab; to Grant for

always bringing a calm and reassuring presence; to Apisata for your wonderful smile and spring rolls. Thank you to the incoming lab members, Josh, Ethan, Ryan, and Michael, for letting me know the lab is in good hands. And of course Evan, who is one of the most intelligent, caring people I have ever met, and was always there to help. I give special thanks to Jess, who was my first mentor at lab, and whom I now consider one of my best friends. Your teachings, advise, and encouragement mean more to me than you will ever know, you are an inspiration to me, and I am so very proud of everything that you do. Lastly, to my sister and partner in crime, Caitlin Cato, whose friendship has changed my life for the better; you are such a wonderful, loving, and caring person, and I am so happy that we had each other's back no matter what challenges we faced. Thank you both for your support and love, your encouragement means the world.

TABLE OF CONTENTS

Page

LIST OF TABLES

Page

LIST OF FIGURES

Page

CHAPTER 1

INTRODUCTION AND LITERATURE REVIEW

Industrial Application of Functional Coatings

Product manufacturing is continuously evolving in a competitive marketplace to increase assets such as product quality, delivery speed, manufacturing cost, and excellent customer service.[1] Manufacturing processes can consist of a multitude of steps, each with opportunities for advancement. For example, night vision goggles, an advanced piece of military equipment, have ten major processes for manufacturing: generation of curvature, blocking, grinding, polishing, frozen separation, ultrasonic cleaning, inspecting, centering, vacuum coating, and cementing.[1] High performance eye wear, because of its laborious manufacturing process, is a particularly important area of research both for improving the quality of the product and for streamlining production methods. One such possibility for eyewear improvement comes in the form of functional polymer coatings, which can offer decoration, protection, and special functionality such as antifogging or self-cleaning.[2] These specialty coatings are not made through traditional synthesis methods or formulation techniques, but can be actualized through the use of functional polymers. Collaboration and integration of scientific research in commercial manufacturing is necessary for product development. The challenge for researchers is integrating new technologies in a way that conforms to preexisting production methodologies, such as industry substrate preferences, manufacture line coating, and irradiation capabilities.

Anti-Fog Polymer Coatings

Functional coatings are useful for many applications and offer specific desirable qualities, such as wettability, barrier properties, adhesion, and bonding ability. One application of specific interest is anti-fog surface modifications. Formation of fog due to water vapor condensation resulting from change in temperature or humidity leads to problems in practical application. Anti-fog coatings are not limited to high performance eyewear, they are also used in windshields, optical instrumentation, and mirrors.[3-7] There are many different ways to create antifogging films with surface modification such as deposition of hydrophilic nanoparticles or textured films, but a promising candidate, due to low cost and simplicity, are hydrophilic polymer coatings. Hydrophilic surfaces allow water droplets to spread uniformly and form a thin water film, reducing light scattering.[8] For instance, Chevallier, et al. developed a polymer anti-fog coating by spin coating poly(ethylene-maleic anhydride) (PEMA) and poly(vinyl alcohol) (PVA) that delayed fog formation and decreased the rate of light transmission decay. Yeh, et al. silanated a zwitterionic sulfobetaine silane (SBSi) onto an oxidized surface to create a hydrophilic surface with significant anti-fog and self-cleaning properties. A very promising candidate for a facile and economical functional coating is a zwitterionic copolymer that exhibits excellent antifogging properties.[9]

The copolymer (BPMPC) consists of a zwitterionic monomer (2-methacryloyloxyethyl phosphorylcholine (MPC)) that provides high hydrophilicity, and a benzophenone moiety to produce a densely crosslinked network.[9] It is easily synthesized, and demonstrates excellent antifogging (Figure 1.1) and self-cleaning capabilities. Its ability to solvate in ethanol makes it compatible for use with plastic eyewear and environmentally friendly. In addition, chemical and mechanical resistance was exhibited by the crosslinked coating. BPMPC is a prime candidate for

commercial manufacturing of high-performance antifogging eyewear. However, there are potential limitations that must be overcome, such as scaling synthesis and optimization of coating methods.

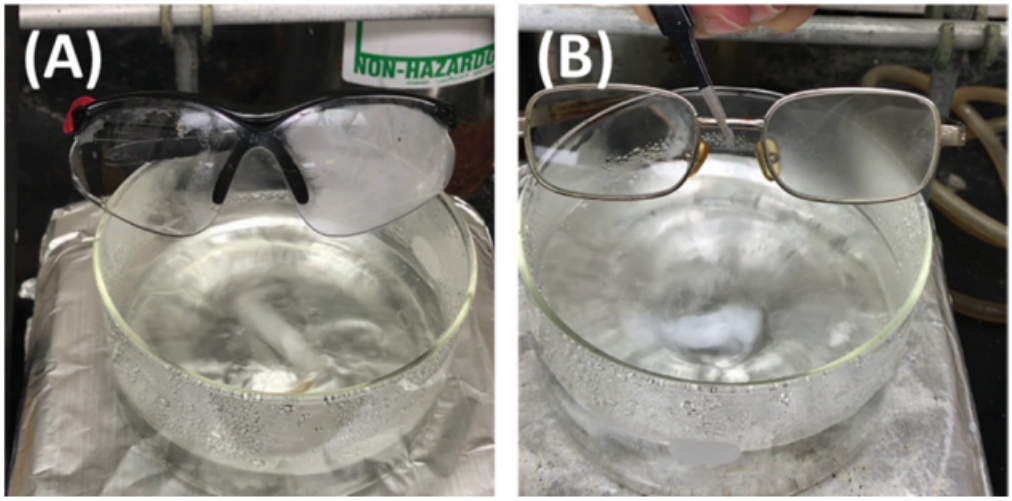

Figure 1.1 Photographs of (A) polycarbonate safety glasses and (B) eyeglasses on hot boiling water (left sides with BPMPC coating).[23]

Benzophenone as a Photo-Crosslinker

Biradical Triplet Formation

Photoreactive reagents are widely used for polymer functionalization of surfaces, including diazirines[10], aryl azides[11,12], nitrobenzils[13,14], cyclic disulfides[15,16], and benzophenone (BP).[9,17,18] BP possesses unique photochemical properties, is a versatile crosslinker, and is commercially available, making it one of the most widely used photo-crosslinkers in biochemistry, organic chemistry, and material science.[19-21] Upon UV irradiation , two possible excited singlet (S_1, S_2) and triplet states (T_1, T_2) can be achieved (Figure 1.2).[22] A π electron from the bonding orbital can be excited to the lowest-energy unoccupied orbital, π^*, making the $\pi -$

π^* transition. The nonbonded n electrons, found on the carbonyl oxygen, can also be excited to the π^* orbital, making what is known as the $n - \pi^*$ transition. It is important to note that these transitions are the excitation from ground state (S_0) to singlet states (S_1 and S_2). As shown in Figure 1.2, intersystem crossing (ISC) from the singlet state (S_1) to triplet state (T_1 and T_2) can occur upon the electron spin configuration changing from a multiplicity of 1 to 3. A direct transition from S_0 to T_1 is spin forbidden by El-Sayed rules.[23] Transition between S_2 and T_2 is not energetically favorable, however rapid ISC can take place between the S_1 and T_2 since they have been shown to be isoenergetic.[24]

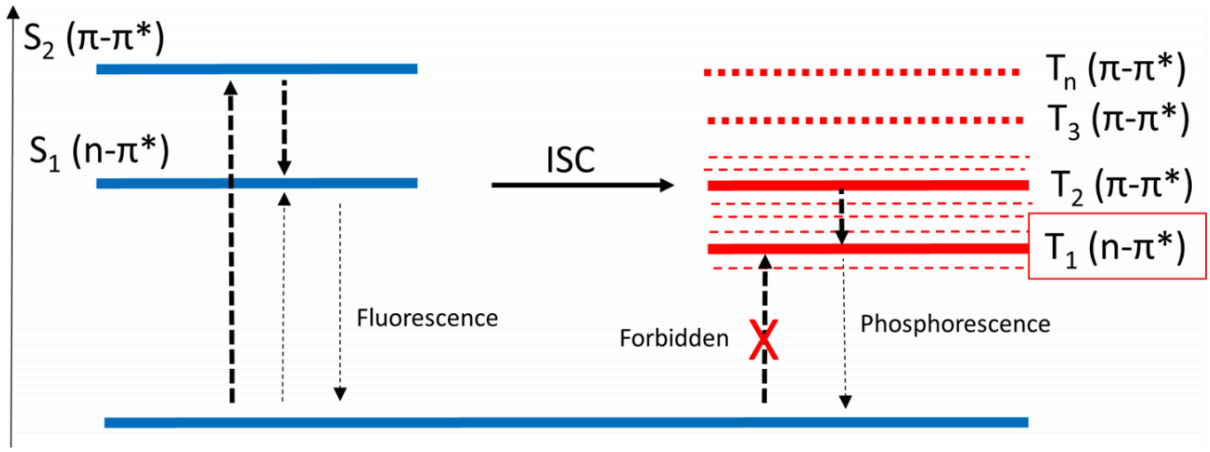

Figure 1.2 Jablonski diagram of Benzophenone excited states.[22]

The T_1 state is known to be a diradical responsible for abstraction of aliphatic hydrogens with high reactivity, whereas the T_2 excited state creates a radical in the aromatic conjugated pi system (Figure 1.3).[19] There are conflicting reports regarding T_2 state and if T_2 acts as an intermediary step between S_1 and T_1[19], or if the electrons can also remain in the excited T_2 state and react directly from that configuration.[25] The $n - \pi^*$ triplet is the most reactive of the excited state species in BP, while $\pi - \pi^*$ is the least reactive.[22] The lifetime of the triplet state can vary

based on the reactivity of the media[26] and the substitution pattern on the aryl ring.[27] Most important to the benzophenone crosslinking chemistry is the $n - \pi^*$ transition because hydrogen abstraction occurs from this electron configuration. It is important to note that $\pi - \pi^*$ transitions are likely to occur at a greater rate due to the spatial proximity of the n and π electrons to the excited π^* state.

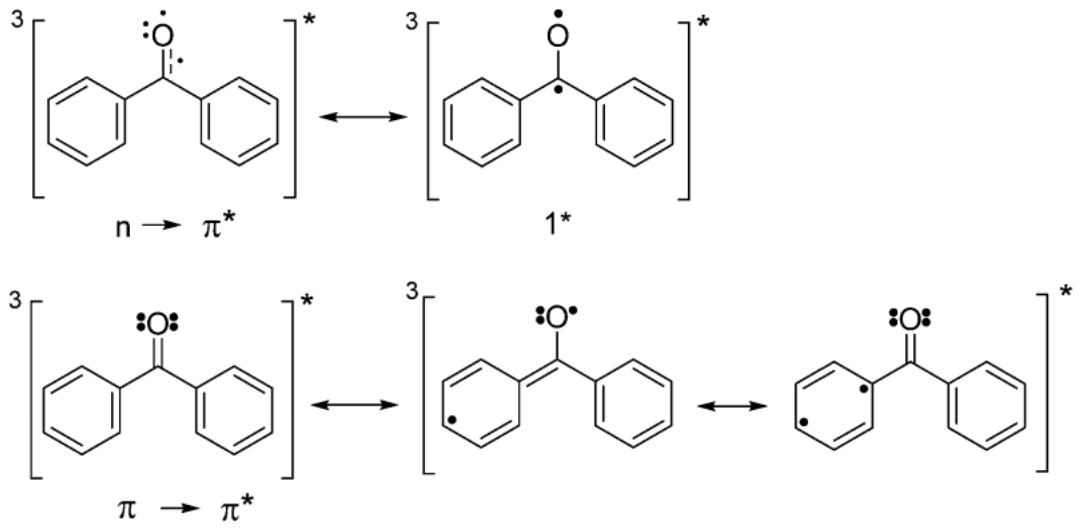

Figure 1.3 Triplet states of BP with resonance structures.[22]

Hydrogen Abstraction and Crosslinking of Benzophenone

The hydrogen abstraction mechanism of benzophenone allows for the crosslinking of the BP moiety to an available C-H bond upon irradiation. The $n - \pi^*$ biradicaloid triplet state can abstract a hydrogen atom from accessible C-H bonds, allowing for the subsequent radicals to recombine and create stable, covalent C-C bonds (Figure 1.4). This photo-reaction allows for various approaches to surface modification in polymer and material science. However, hydrogen abstraction by benzophenone is dependent on the reactivity, density, and location of the

abstractable hydrogens.[28] Radical stability is the primary kinetic driver for hydrogen abstraction with reactivity decreasing as radical stability decreases.[29] Aliphatic hydrogens located alpha to heteroatoms such as nitrogen display increased reactivity due to charge transfer interactions between the BP triplet and electrons in the heteroatom prior to abstraction.[28] Radical stability generally increases with increasing substitution, therefore kinetics for abstraction increase in the order of primary, secondary, and tertiary hydrogens. Aromatic hydrogens are among the least reactive, with a rate constant two orders of magnitude lower than primary hydrogens.[30]

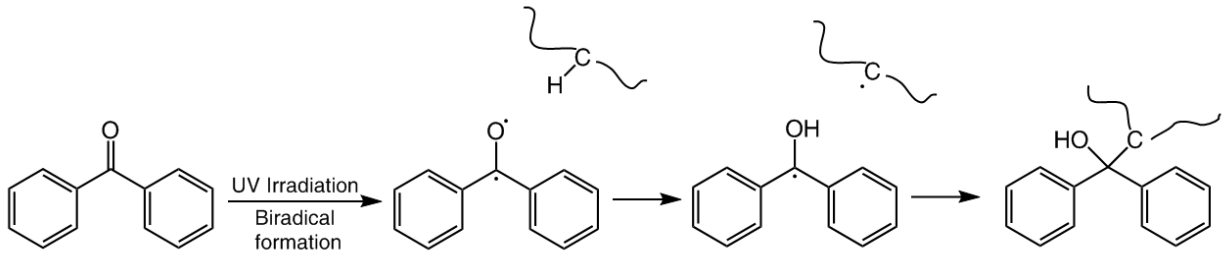

Figure 1.4 Scheme of benzophenone (BP) hydrogen abstraction and crosslinking.

Oxidation and Photobleaching

Photoinduced degradation (photobleaching) and oxidation remain an important factor for chromophores that undergo UV irradiation. One of the main components of oxidation[31] and photobleaching[32-36] is the formation of reactive oxygen species (ROS), which is a collective term for singlet oxygen, superoxide radicals, and any other oxidizing species formed subsequently.[37] Molecular oxygen can react with BP in the biradical triplet state to form ROS and subsequently degrade chromophores.[37-39]

Hou et al. studied ROS production under UV light exposure in a photoactive benzophenone derivative for the creation of antimicrobial cellulose textile. 3,3',4,4'-Benzophenone tetracarboxylic acid (BPTCA) was reacted with the hydroxyl groups on cellulose to form ester bonds, and the photochemical reactive mechanism was investigated (Figure 1.5). The triplet state of benzophenone is achieved through UV irradiation, after intersystem crossing (ISC) from the excited singlet state. The benzophenone intermediate triplet state can be readily quenched by oxygen to the ground state with the production of singlet oxygen ($^1O_2$), or it can abstract a hydrogen atom from another molecule, generating a benzophenone radical and carbon radical, which then may undergo crosslinking via an alternative pathway previously discussed (Figure 1.5, reactions 1-3).[40,41] Under continuous light exposure, the benzophenone radical can react with oxygen to produce ROS, such as hydroxyl radicals ($HO^{\cdot}$), superoxide ($O^{\cdot}$), and hydrogen peroxide (H_2O_2) (Figure 1.5, reactions 4-7). ROS concentrations, specifically hydrogen peroxide) were shown to increase with increasing irradiation exposure, but were not effect by temperature during irradiation.

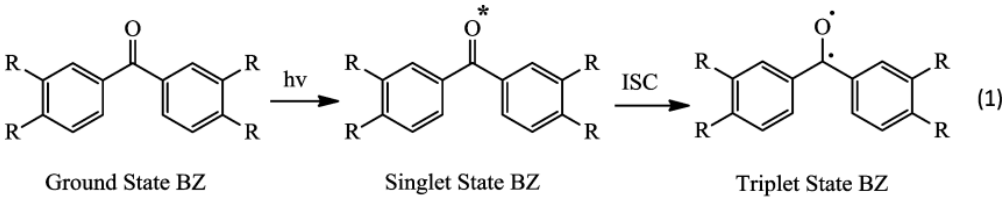

(1)

BZ = benzophenone

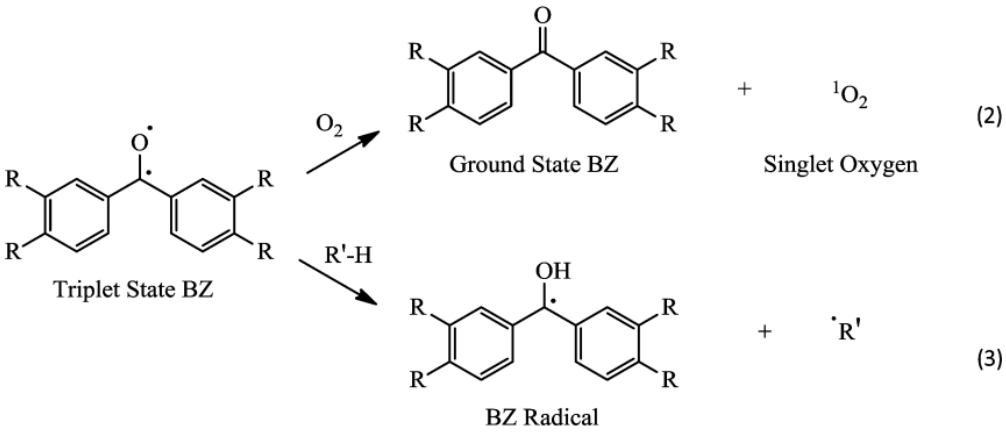

(2)

(3)

R' =Cellulose-O group

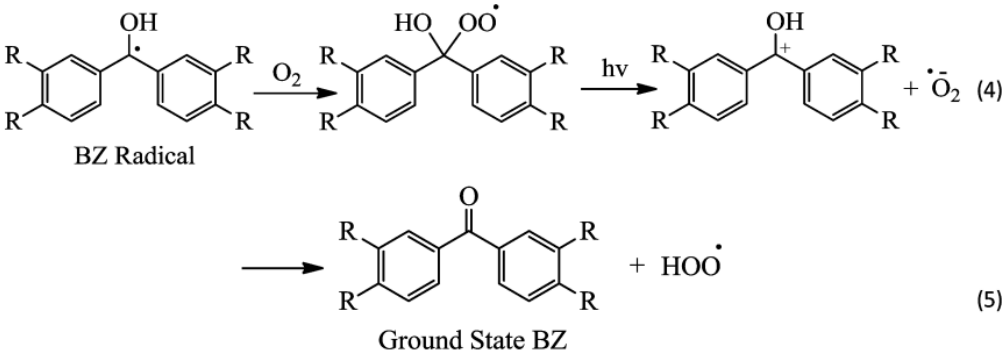

(4)

(5)

$$2HOO^{\bullet} \longrightarrow H_2O_2 + O_2 \quad (6)$$

$$H_2O_2 + {}^{\bullet}O_2^{-} \longrightarrow {}^{\bullet}OH + {}^{-}OH + O_2 \quad (7)$$

Figure 1.5 Scheme of Benzophenone Photoactive Reaction[42]

Thesis Objectives

The objective of this thesis is to further the understanding of the BPMPC polymer system and its potential limitations as a commercially viable functional coating. This was completed by rigorous fog and abrasion testing to determine optimal properties necessary for high-performance eyewear. The effects of residual monomer on these properties necessitated the addition of a secondary precipitation step during synthesis to enable a densely crosslinked network. In addition, substrates containing abstractable hydrogens with different radical stability were evaluated to define the ability of BPMPC to crosslink to commercially utilized substrates. Lastly, kinetics of reaction were investigated by UV-Visible spectroscopy (UV-Vis) and Fourier transform infrared spectroscopy (FTIR), where it was determined photobleaching and oxidation interference had occurred.

References

1. Chen, K. H., M.; Chang, P., Performance evaluation on manufacturing times. *Int J Adv Manuf Technol* **2005,** *31*, 335-341.

2. Wu, L. B., J., Functional Polymer Coatings: Principle Methods and Applications Preface. *Wiley Ser Polym Eng* **2015**, Xiii-Xiv.

3. Chevallier, P. T., S.; Sarra-Bournet, C.; Turcotte, R.; Laroche, G., Characterization of Multilayer Anti-Fog Coatings. *2011* **2011,** *3*, 750-758.

4. Howarter, J. A. Y., J. P., Self-Cleaning and Next Generation Anti-Fog Surfaces and Coatings. *Macromol. Rapid Commun.* **2008,** *29*, 455-466.

5. Petit, J. B., E., General Frost Mechanism on Solid Substrates with Different Stiffness. *Langmuir* **2014,** *30*, 1160-1168.

6. Wang, Y. L., T. Q.; Li. S. H.; Sun, J. Q., Antifogging and Frost-resisting Polyelectrolyte Coatings Capable of Healing Scratches and Restoring Transparency. *Chem. Mater.* **2015,** *27*, 8058-8065.

7. Zhao, J. M., A.; Ma. L.; Wang, X. J.; Ming, W. H., Terpolymer-based SIPN Coating with Exellent Antifogging and Frost-Resisting Properties. *RSC Adv.* **2015,** *5*, 102560-102566.

8. Huang, W. C., Y.; Yang, C.; Situ, Y.; Huang, H., PH-driven phase separation: Simple routes for fabricating porous TiO2 film with superhydrophilic and anti-fog properties. *Ceram. Int.* **2015,** *41*, 7573-7581.

9. Liu, Q. L., J., Transparant Grafted Zwitterionic Copolymer Coatings That Exhibit Both Antifogging and Self-Cleaning Properties. *ACS Omega* **2018,** *3* (12), 17743-17750.

10. Sinz, A., Chemical Cross-linking and Mass Spectrometry to Map Three-Dimensional Protein Structures and Protein-Protein Interactions. *Mass Spectrom Rev* **2006,** *25* (4), 663-682.

11. Tanaka, Y. B., M. R.; Kohler, J. J., Photocrosslinkers Illuminate Interactions in Living Cells. *Mol Biosyst* **2008,** *4* (6), 473-480.

12. Pham, N. D. P., R. B.; Kohler, J. J., Photocrosslinking Approaches to Interactome Mapping. *Curr Opin Chem Biol* **2013,** *17* (1), 90-101.

13. Nam, C. Y. Q., Y.; Park, Y. S.; Hlaing, H.; Lu, X.; Ocko, B. M.; Black, C. T.; Grubbs, R. B., Photo-Cross-Linkable Azide Functinalized Polythiophene for Thermally Stable Bulk Heterojunction Solar Cells. *Macromolecules* **2012,** *45* (5), 2338-2347.

14. Yoo, M. K., S.; Lim, J.; Kramer, E. J.; Hawker, C. J.; Kim, B. J.; Bang, J., Facile Synthesis of Thermally Stable Core-Shell Gold Nanoparticles via Photo-Cross-Linkable Polymeric Ligands. *Macromolecules* **2010,** *43* (7), 3570-3575.

15. Guo, L. W. G., J. E.; Hajipour, A. R.; Muradov, H.; Arbabian, M.; Artemyev, N. O.; Ruoho, A. E., Asymmetric Interaction Between Rod Cyclic GMP Phophodiesterase Gamma Subunites and Alpha Beta Subunits. *J Biol Chem* **2005,** *280* (13), 12585-12592.

16. Suga, T. K., H.; Nishide, H., Photocrosslinked Nitroxide Polymer Cathode-Active Materials for Application in an Organic-Based Paper Battery. *Chem Commun* **2007,** *17*, 1730-1732.

17. Liu, Q. L., J., Photocross-linking Kinetics Study of Benzophenone Containing Zwitterionic Copolymers. *ACS Omega* **2020**.

18. Liu, Q. S., P.; Handa, H.; Locklin, J., Covalent Grafting of Antifouling Phosphorylcholine-based Copolymers with Antimicrobial Nitric Oxide Releasing Polymers to Enhance Infection-Resistant Properties of Medical Device Coatings. *Langmuir* **2017,** *33* (45), 13105-13113.

19. Dorman, G. P., G. D., Using Photolabile Ligands in Drug Discovery and Development. *Trends Biotechnol.* **2000,** *18*, 64−77.

20. Horie, K. A., H.; Mita I., Photochemistry in Polymer Solids (8) Mechanism of Photoreaction of Benzophenone in Polyvinyl-Alcohol. *Macromolecules* **1987,** *20* (1), 54-58.

21. Brauchle, C. B., D. M.; Bjorklund, G. C., Hydrogen Abstraction by Benzophenone Studied by Holographic Photochemistry. *J Phys Chem-Us* **1981,** *85* (2), 123-127.

22. György Dorman, H. N., Abigail Pulsipher, and Glenn D. Prestwich, The Life of Pi Star: Exploring the Exciting and Forbidden Worlds of
the Benzophenone Photophore. *ACS, Chemical Reviews* **2016,** *116*, 15284−15398.

23. El-Sayed, M. A., Triplet state. Its Radiative and Nonradiative Properties. *Acc. Chem. Res.* **1968,** *1*, 8−16.

24. Yabumoto, S. S., S.; Hamaguchi, H.-O., Vibrational and Electronic Infrared Absorption Spectra of Benzophenone in the Lowest Excited Triplet State. *Chem. Phys. Lett.* **2005,** (416), 100−103.

25. Marazzi, M. M., S.; Roca-Sanjuan, D.; Delcey, M. G.; Lindh, R.; Gonzalez, L.; Monari, A., Benzophenone Ultrafast Triplet Population: Revisiting the Kinetic Model by Surface-hopping Dynamics. *J. Phys. Chem. Lett.* **2016,** *7*, 622-626.

26. Takahashi, K. T., H.; Kitamura, S.; Satoh, T.; Katoh, R, Reactions of Excited-State Benzophenone Ketyl Radical in a RoomTemperature Ionic Liquid. *Phys. Chem.* **2010,** *12*, 1963-1970.

27. Turro, N. J. R., V.; Scaiano, J. C., *Principles of Molecular Photochemistry: an Introduction* **2009**.

28. Christensen, S., *Macromolecules* **2012,** *45*, 5237-5246.

29. Wagner, P. P., B., Photoinduced hydrogen atom abstraction by carbonyl compounds. *Org. Photochem* **1991,** *11*, 227-366.

30. Giering, L. B., M.; Steel, C., Rate Studies of Aromatic Triplet Carbonyls with Hydrocarbons. *J. Am. Chem. Soc.* **1974,** *96*, 953-958.

31. Lee, M. L., H.; Han, S.; Kim, H.; and Won, Y., Photo-oxidation in the photobleaching process of a non-linear optical polymer. *Thin Solid Films* **1996,** *283*, 247-250.

32. Brinkmann, T. S., D.; and Frimmel, F., Photobleaching of Humic Rich Dissolved Organic Matter. *Aquat. Sci.* **2003,** *65*, 415-424.

33. Bonnett, R. a. M., G., Photobleaching of sensitisers used in photodynamic therapy. *Tetrahedron* **2001,** *57*, 9513-9547.

34. Chen, P. L., J.; Qian, Z.; Okasaki, T.; and Hayami, M., Study on the photooxidation of a near-infrared-absorbing benzothiazolone cyanine dye. *Dyes Pigm.* **1998,** *37*, 213-222.

35. Byers, G. G., S.; and Henrichs, P., Direct and Sensitized Photoxidation of Cyanine Dyes. *Photochem. Photobiol.* **1976,** *23*, 37-43.

36. Kuramoto, N. a. K., T., The contribution of singlet oxygen to the photofading of triphenylmethane and related dyes. . *Dyes Pigm.* **1982,** *3*, 49-58.

37. Zheng, Q. J., S.; Zhou, Z.; and Blanchard, S. , The Contribution of Reactive Oxygen Species to the Photobleaching of Organic Fluorophores. *Photochemistry and Photobiology* **2014,** *90*, 448-454.

38. Fengel, D. W., G., *Wood-Chemistry, Ultrastructure, Reactions*. Walter de Gruyter: Berlin, 1984.

39. Lanalunga, O. B., M., Photo- and Radiation Chemical Induced Degradation of Lignin Model Compounds. *J. Photochem. Photobiol.* **2000,** *56*, 85-108.

40. Anslyn, E. D., D., *Modern Organic Chemistry*. University Science Books: Sausalito, CA, 2006.

41. Liu, N. S., G., Production of Reactive Oxygen Species by Photoactive Anthraquinone Compounds and Their Applications in Wastewater Treatment. *Ind. Eng. Chem.* **2011,** *50*, 5326-5333.

42. Hou, A. F., G.; Zhuo, J.; Sun, G., UV Light-Induced Generation of Reactive Oxygen Species and Antimicrobial Properties of Cellulose Fabric Modified by 3,3',4,4'-Benzophenone Tetracarboxylic Acid. *ACS Appl. Mater. & Interfaces* **2015,** *7*, 27918-27924.

CHAPTER 2

EVALUATION OF ANTI-FOG PROPERTIES, ABRASION RESISTANCE, AND KINETICS OF REACTION FOR A ZWITTERIONIC FUNCTINAL COATING[1]

[1]Smith, M. and Locklin, J. To be submitted to *ACS Omega*.

Abstract

In this work, we investigated a zwitterionic copolymer as a viable and commercially scalable option for use as anti-fog coatings for high performance eyewear. The polymer coatings were photochemically grafted to available abstractable hydrogens on substrates via a benzophenone moiety to produce a robust crosslinked network. Evaluation of the applicability and performance of this polymer were imperative, so a series of experiments investigating the anti-fogging properties, abrasion resistance, and kinetics of crosslinking were performed. It was determined that crosslinking was affected by monomer impurity, leading to an additional purification step for larger scale synthesis. It was determined that substrates possessing hydrogens that are abstracted at rates slower than those within the polymer chain are not viable for creation of high-performance eyewear. Additionally, the kinetics of crosslinking were found to be affected by the wavelength of irradiation. Photobleaching and oxidation of the benzophenone occurred during irradiation in the presence of an oxygenated atmosphere. Issues with commercial application were addressed and improved, resulting in a more viable anti-fogging, abrasion resistant coating for high performance eyewear.

Introduction

Tremendous effort has gone into the development of functional surfaces through manipulation of chemical and physical properties to achieve optimal interfacial reactions for various applications in biotechnology, optics, electronics, and photonics.[1-5] One subsection of specific interest is functionalized surfaces that possess anti-fogging properties. This is achieved by limiting the water vapor condensation formation resulting from temperature and humidity changes, therefore solving practical problems in applications such as windshields, optical instruments, safety and eyeglasses.[6-10] There are many different ways to create anti-fogging films, such as electro-spinning a textured film, which facilitates the spread of water via modifying the surface's chemical environment and geometric microstructure.[11-14] Other methods include deposition of hydrophilic photo-activated TiO_2 and ZnO nanoparticles,[15-17] or a hydrophilic polymer coating.[18, 19] Toxicity of reagents, added costs for multi-step production, and robustness of final product are practical limitations, which provide the basis for methodology selection.

Among all methods, use of the zwitterionic polymer BPMPC was deemed a cost efficient, versatile, and an environmentally friendly choice for creation of a hydrophilic anti-fogging polymer film. Previous research has shown that[18, 19] MPC's charged groups create a hydration shell as a result of electrostatic interactions similar to that of free water, which provides the optimal anti-fogging properties displayed by zwitterionic polymers. Robustness of the anti-fogging polymer film is achieved via incorporation of benzophenone (BP) on the polymer backbone, which acts as a crosslinking agent. Synthesis and structure of BPMPC is shown in Figure 2.1. UV Irradiation can cause multiple excitation transitions, including $n - \pi^*$ and $\pi - \pi^*$ excitations, allowing for the abstraction of hydrogen atoms from neighboring C-H bonds to form new C-C bonds.[20] The use of BP offers many benefits including rapid

photochemical reactions and the ability to tailor UV irradiation parameters for adjusted surface properties.[21, 22]

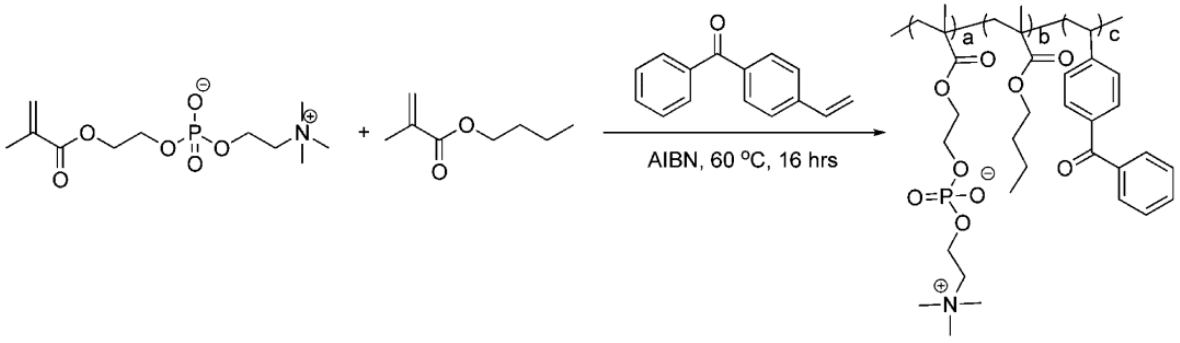

Figure 2.6 Synthesis of BPMPC Copolymer[23]

While BP is a very versatile and apt choice for anchoring anti-fogging zwitterionic polymer films, there are limitations to both laboratory scale processes and commercial upscaling that must be considered. For example, Christensen et al. analyzed the gelation of acrylate copolymers with pendent BP UV-induced crosslinkers, and found that the location and type of highly abstractable hydrogen atoms were crucial to the ability of BP to create robust networks. When the abstractable hydrogens were present on the main polymer chain, BP induced chain scission rather than crosslinking, and the species of hydrogen dictated the rate constants for abstraction.[24] Limitations on type of plastic substrate available to create a robustly crosslinked network is of special importance for industrial application. The most common plastic used for goggles is polycarbonate, with nylon, a more durable option, being considered for newer models. For the industrial application of anti-fog coating, the type of plastic used, as well as any previous surface functionalization such as anti-abrasion coatings, must be considered. In addition, although BP hydrogen abstraction reaction has been shown to be proceed with reasonable

efficiency in the presence of oxygen,[25, 26] there are indications of oxidation and photobleaching.[27-30] This not only effects the ability to monitor the reaction via spectroscopy, but it also effects the capacity of BP to create robust polymer networks.

In this study, a zwitterionic copolymer (2-methacryloyloxyethyl phosphorylcholine-co-butyl methacrylate-co-benzophenone, BPMPC) was synthesized and covalently grafted to alkyl-modified glass and plastic eye lenses upon UV-irradiation. The potential limitations of BPMPC coatings on anti-fogging and abrasion resistance were characterized, leading to a greater understanding of the polymer system and its potential application in industry. The BPMPC coating performance showed sensitivity to monomer impurities, thus introducing additional purification steps during synthesis. Limitations for commercial use also include the type of plastic lens and the abstractable hydrogens it contains. There must be a greater affinity for polymer-substrate over polymer-polymer crosslinking in order to achieve a robust network able to withstand normal eyewear abrasion. Moreover, optimal irradiation parameters including wavelength and atmosphere were evaluated for their effect on kinetics and oxidation.

Experimental Section

Materials

2-Methacryloyloxyethyl phosphorylcholine (MPC) was purchased from Sigma Aldrich; 2,2'-azobis(2-methylpropionitrile) (AIBN) and n-butyl methacrylate (BMA) were purchased from Alfa-Aesar. Isobutyltrichlorosilane (iBTS) was purchased from Tokyo Chemical Industry. Glass slides were purchased from Fisher-Scientific. All sample goggles, polycarbonate, and nylon were supplied by US Army Combat Capabilities Development Command Soldier Center in Natick, MA.

Synthesis of 4-vinyl benzophenone (4-VBP)[23]

In a flame dried round bottom flask, 1M magnesium chlorostyrene is prepared by dissolving excess magnesium and p-chlorostyrene in THF with a flake of iodine. 1 equiv. of benzonitrile is then added dropwise, followed by stirring for 6 hours. The mixture was cooled to 0°C and quenched with water, followed by dilute sulfuric acid until a homogeneous solution was obtained. The solution was subjected to an aqueous workup and dried with $MgSO_4$. After removal of the solvent, the crude product was purified by flash chromatography. The resulting residue was further purified by trituration from MeOH once, followed by EtOH twice, affording a 41% yield.

Synthesis of BPMPC

All BPMPC polymers were synthesized by radical polymerization using a previously reported procedure.[18] In general terms, MPC, BMA, and 4-VBP were dissolved in EtOH (total monomer concentration of 1 mmol mL^{-1}) with AIBN initiator (concentration of 0.01 mmol mL^{-1}) and degassed in argon for approximately 30 minutes. The radical polymerization reaction was carried out under N_2 atmosphere at 60°C for 16 h. Reaction was completed by cooling, exposing to air, and precipitating in ethyl ether. It was then dried under vacuum for 12 h to gain white solid product. Structure and monomer ratio were confirmed by ^1H NMR in DMSO (Figure A1, Table A1).

Substrate Preparation and BPMPC Coating

All glass slides, quartz, and silicon substrates were sonicated with deionized water, isopropanol, acetone, and hexane for 5 minutes each, then dried under nitrogen. They were plasma cleaned (Harrick Plasma PDC-32G) and treated with iBTS dissolved in toluene overnight, before being rinsed and dried under nitrogen.

Spin coating, drop casting, and paint coating were all used for application onto the substrate. For spin coating, 0.25 mL of BPMPC/ethanol solution (10 mg mL^{-1}) was spun at 1000 rpm for 30 seconds. Drop casting was used for quartz substrates during UV-Vis kinetics studies. Paint coating was applied to goggles and other substrates with a sponge paint brush at a concentration of 10 mg mL^{-1}. The coating was applied by wetting the brush in solution, and pulling across once to gain a uniform and even coating. Solvent was allowed to evaporate, and another coating was applied for a total of 4 passes. Irradiation was performed with a wavelength of 254 nm or 365 nm.

Characterization of Polymer Coatings[23]

UV-Vis Spectroscopy and Kinetic Measurements

Benzophenone crosslinking was evaluated with UV-Vis spectroscopy on iBTS functionalized quartz substrates. The decreasing intensity of the BP carbonyl during reaction completion was used for kinetics calculations. The polymer solution (10 mg mL^{-1}) was cast on functionalized quartz and allowed to evaporate. The UV-Vis spectroscopy was performed on a Cary Bio spectrophotometer (Varian) and irradiation was completed using a Compact UV Lamp (UVP) with a wavelength of 254 nm and 365 nm. The substrates were held a specific distance from the light to obtain approximately 6.5 mW cm^{-2} for both wavelengths of irradiation.

Inert atmosphere was created by clamping a 1 in x 1 in custom mold with rubber O-rings between the BPMPC coated quartz and a blank quartz. This mold had a needle inlet for nitrogen flow, and was monitored by needle outlet into a water bath, with a bubble production of approximately 1 per second. The inert quartz chamber was allowed to purge for 5 minutes before UV-Vis measurements were taken. Irradiation was completed by placing the UV lamp inside the UV-Vis instrument, to ensure that the substrate was not moved in between measurements.

Infrared Spectroscopy (GATR-FTIR)

Thermo-Nicolet model 6700 spectrometer equipped with a variable grazing angle attenuated total reflection (GATR) accessory (Harrick Scientific) was used for infrared spectroscopic studies. Resolution was set to 2, with spectra taken between 4000 and 600 cm^{-1}. A 5 μL BPMPC/EtOH solution (10 mg mL^{-1}) was drop casted directly onto the Ge crystal and allowed to evaporate to remove all ethanol. In between FTIR measurements, irradiation was directly applied to the coating while on the Ge crystal. Inert atmosphere was created by modifying the set up used in UV-Vis spectroscopy. The custom mold and one quartz slide were clamped to the coated Ge crystal, and allowed to purge for 5 minutes before measurements and irradiation via UV lamp were completed. A water bath and outlet hose were used to monitor nitrogen flow.

Anti-fogging Test[19]

The anti-fogging property of various BPMPC coated substrates were evaluated by hot-vapor methods. The coated substrates' optical clarity was qualitatively evaluated by T-40-1-P-OP NBS-1952 Resolution Test Chart before and after being held approximately 3 cm above 60°C water for 20-30 seconds. Pass/Fail evaluation was determined by the level of optical clarity seen. Videos and photographs were recorded for each experiment.

Abrasion Test

Abrasion testing kit was purchased form EMS Acquisition Corp, consisting of a MIL-CCC-C-440 cheesecloth and 1-1.25 lb aluminum abrasion tester. MIL-M-13508C, 4.4.5, MIL-C-675C 3.8.4.2 and 4.5.11 were followed for testing the coatings optics and abrasion. Generally, this consisted of securing a folded 3"x4" piece of cheesecloth over the eraser, located at the tip of the aluminum tester. The tester was held normal to substrate and cycled back and forth for 25

cycles, or 50 strokes, over an area of approximately 1 inch. The substrate was then cleaned, dried, and optically inspected for any deviations between abraded and non-abraded surfaces. In addition, anti-fogging properties were re-evaluated to ensure fogging performance was not affected during abrasion of BPMPC coating.

Results and Discussion

1. Monomer Impurity

The importance of polymer purity and its effect on BPMPC performance, such as anti-fogging abilities and abrasion resistance, is studied in this section. On both a commercial and laboratory scale, the impact of residual monomer in the zwitterionic copolymer system can be detrimental to coating performance. Therefore, it is important to understand what effects impurities can impose in order to create optimal coating performance.

Previous research showed[23] a zwitterionic copolymer (benzophenone-co-2-methacryloyloxyethyl phosphorylcholine-co-butyl methacrylate, BPMPC) possessing anti-fogging properties[19] was synthesized by radical polymerization, and polymer composition was confirmed using ^{1}H NMR spectroscopy (Figure A1). Monomer composition was based on NMR integrations[23] for 3.25 ppm (-N(CH_3)$_3$, 9H) for the MPC unit, 1.45-1.63 ppm (-CH_2-, 4H) for the BMA unit, and 6.80-7.85 ppm (aromatic C-H, 9H) for the BP unit. While precipitated after synthesis, ^{1}H NMR spectroscopy did show residual monomer, therefore further purification via multiple precipitations (ethanol into ether) was conducted for a purified BPMPC (Figure A2). Overall composition of monomer units remained relatively consistent between BPMPC and BPMPC-RM (residual monomer), as outlined in Table A1. In addition, kinetics of irradiation for BPMPC was unaffected by purification and residual monomer impurity, as shown in Figure B1.

Optical clarity, according to visual inspection using a T-40-1-P-OP NBS-1952 Resolution Test Chart, was unchanged between control, BPMPC-RM and BPMPC coatings.

The anti-fogging performance of BPMPC coatings was demonstrated by hot-vapor tests. It is observed from the images (Figure 2.2) that condensation formed on the noncoated control goggle, and light scattering is easily observed. However, fogging did not occur on the BPMPC functionalized substrates as it was placed over the hot vapor. Excess condensation can sometimes be observed towards the end of fogging tests due to over-saturation of the polymer matrix. The results of this experiment indicate minimal differences between BPMPC-RM and BPMPC, concluding that residual monomer does not affect the performance of the hydrophilic coating nor the ability of the water droplets to diffuse into the polymer coating and expand the basal area, a phenomena that has been shown in previous coatings of semi-interpenetrating polymer networks.[18, 19, 31]

Abrasion resistance is an important component of high-performance anti-fog coatings that is often overlooked. A coating that is not durable to the everyday wear and tear is not useful no matter how well it can prevent fogging. As seen in Figure 2.2, there is a large difference between the abrasion performance of coatings with and without residual monomer. The BPMPC-RM coating immediately abrades under the tester, and fog testing afterwards confirms the permanent removal of the zwitterionic coating. The purified BPMPC does not show any signs of abrasion after testing, demonstrating a robust network of crosslinked polymer with the ability to withstand the daily damage inflicted upon high performance eyewear. It is hypothesized that the excess monomers in the matrix undergo crosslinking during UV irradiation, leading to the BP components linking onto loose molecules, rather than neighboring polymeric chains. Therefore,

the polymer system with residual monomer impurity is not as robust or abrasion resistant as that with minimal monomer concentration.

This is an important consideration for upscaling the zwitterionic copolymer for commercial production, as increased purification through multiple precipitations would be required. This is a facile solution, but may have previously unseen economic impacts in time and solvent costs. The level of tolerable residual monomer impurity is not known, and must be considered for balancing production costs with BPMPC coating performance.

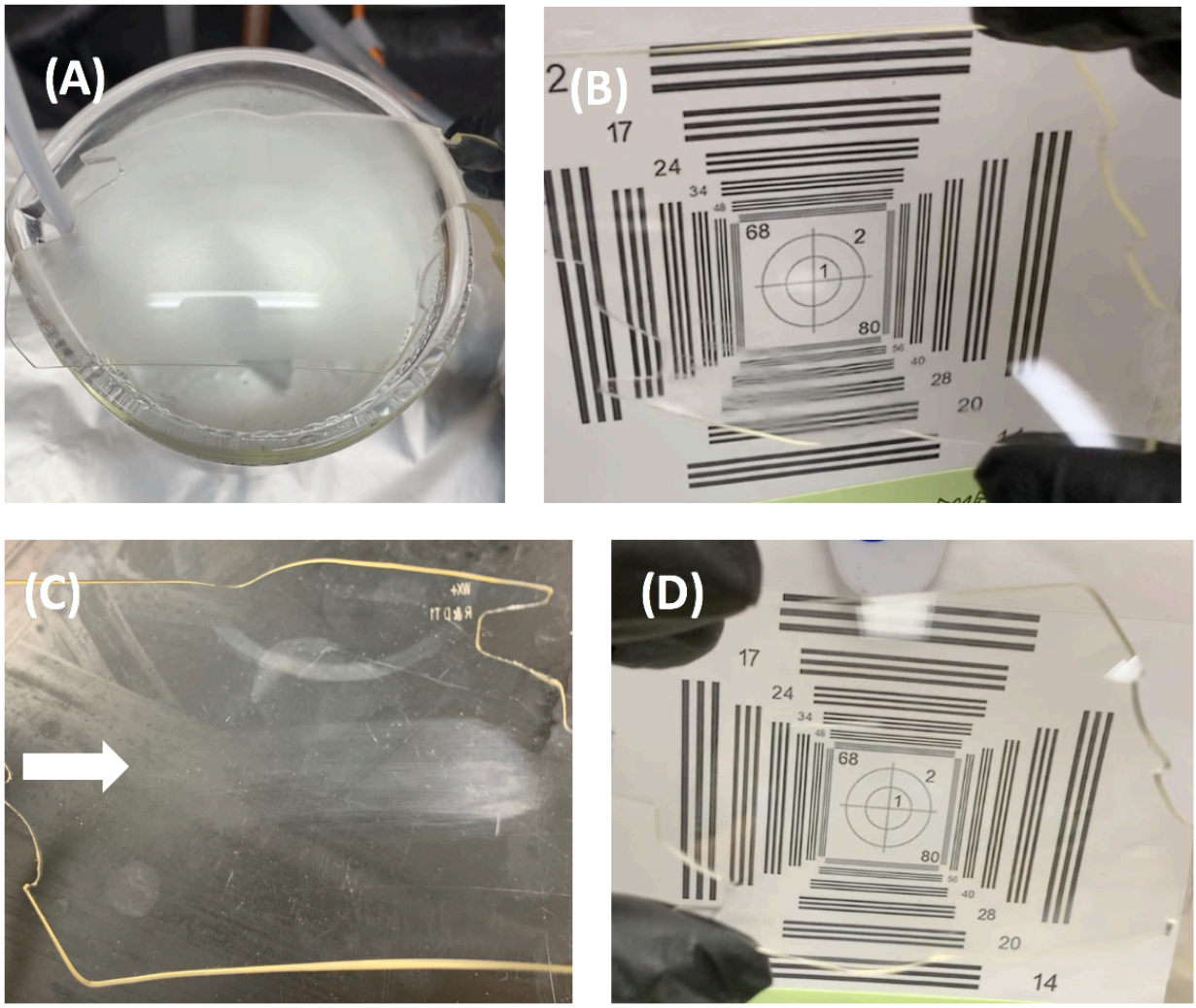

Figure 2.7 Photographs of (A) noncoated goggle over steaming water, BPMPC-RM coated goggle (B) immediately after exposure to the fogging test and (C) after the abrasion test, and (D) BPMPC coated goggle after abrasion and fog testing.

2. Substrate Crosslinking Affinity

As is well studied by Christensen, et. al., the benzophenone chemistry and crosslinking ability is directed by the reactivity, density, and location of abstractable hydrogens in the polymer system. Numerous studies have detailed the reactivity of hydrogens to benzophenone

abstraction, and attribute their sensitivity to radical stability.[24] Certain heteroatoms (for example, nitrogen, oxygen, and sulfur) are particularly susceptible to hydrogen abstraction due to the hcharge transfer interactions between the BP triplet and electrons in the heteroatom.[24, 32, 33] Reaction rates include C-H bonding increase in the order of aromatic, primary (1^0), secondary (2^0), and tertiary (3^0).[24, 34] Reactivity rates, for reference, are outlined in Table 2.1.

Table 2.1 Relative rates of hydrogen abstraction by benzophenone.[24, 34]

species	k [$M^{-1}s^{-1}$]	relative to primary
primary	1.70×10^3	1
secondary	6.8×10^4	40
tertiary	5.1×10^5	300
benzene C-H	2.7×10^1	0.016

It is necessary for the zwitterionic copolymer to successfully crosslink via polymer-substrate linkages to create a robust anti-fogging coating with the ability to withstand normal wear and tear experienced in application. In order for this polymer-substrate linkage to be achieved, the benzophenone must have favorable hydrogen abstractions towards the substrate over the hydrogens located in the polymer itself. The substrate will be favored if the type of hydrogen available has a higher abstraction rate with benzophenone than any hydrogens in the polymer chain. If the substrate has comparable rates of abstraction as the polymer chain, it is hypothesized that crosslinking will occur at equal rates for both polymer-polymer and polymer-substrate. Finally, if the substrate possesses hydrogens that have lower abstraction rates than the

polymer, an imbalance in crosslinking density favoring polymer-polymer linkage will occur, and the coating will not be robust enough to withstand abrasion.

Durability of BPMPC coatings crosslinked to applied substrates were investigated by coating surfaces possessing different abstractable hydrogens, specifically polycarbonate blanks, nylon blanks, and isobutyl trichlorosilane (iBTS) modified glass slides. Polycarbonate and nylon were chosen due to their commonality in eyewear manufacturing. Polycarbonate contains both primary and aromatic hydrogens, while nylon possesses secondary hydrogens (note that the secondary hydrogens are not all equal in reactivity, some are located alpha to a heteroatom causing a differentiation in abstraction rate as stated above). iBTS modified glass slides were chosen for their possession of tertiary, secondary, and primary hydrogens. The coated substrates were irradiated at 254 nm, washed in ethanol to remove excess polymer, and subjected to fogging and abrasion testing.

The zwitterionic BPMPC copolymer contains aromatic, primary and secondary hydrogens, and a single tertiary hydrogen per benzophenone repeat unit. When coated to polycarbonate and irradiated, the benzophenone will undergo hydrogen abstraction at different rates depending on hydrogen reactivity. As shown in Figure 2.3, the BPMPC coated polycarbonate possessed anti-fogging properties, displaying an amount of crosslinking between polymer-substrate to withstand rinsing. However, clear failure was shown upon abrasion testing (Figure 2.3 C), by leaving visible marks and failing the anti-fog test where abrasion occurred. The BPMPC polymer was permanently removed from the substrate, indicating a lack of robust network formation between polymer-substrate. Due to the tertiary and secondary hydrogens in the BPMPC polymer chain, it is unlikely that polycarbonates primary and aromatic hydrogens where able to be abstracted at a rate favorable for the necessary amount of polymer-substrate

crosslinking needed for a robust adherence. It is therefore shown that when the polymer contains hydrogens with a higher abstraction rate, polymer-polymer crosslinking will occur. In terms of coating polycarbonate for eyewear on a commercial scale, one possible solution would be to pre-functionalize the plastic to obtain hydrogens favorable for polymer-substrate interactions. An example of this was shown in section 2.1, in which the polycarbonate sample goggles provided were already pre-coated in proprietary abrasion resistant coatings that allowed for the successful crosslinking of the BPMPC copolymer.

Polymer-substrate interactions were favorable for both nylon and iBTS modified glass, displaying both anti-fogging and abrasion resistant properties (Figure 2.4). Both BPMPC and nylon contain secondary hydrogens available for abstraction. It is shown that a robust crosslinking network necessary to withstand abrasion can be achieved for substrates that contain relatively similar abstraction rates compared to the polymer coating. BPMPC does contain tertiary hydrogens, but it is hypothesized that due to the low density they do not exert enough influence on the overall crosslinking reaction to effect abrasion resistance. The tertiary hydrogens in the iBTS modified glass slide demonstrate that if the substrate contains hydrogens with a greater abstraction rate than the polymer coating, a robust crosslinked network is achieved.

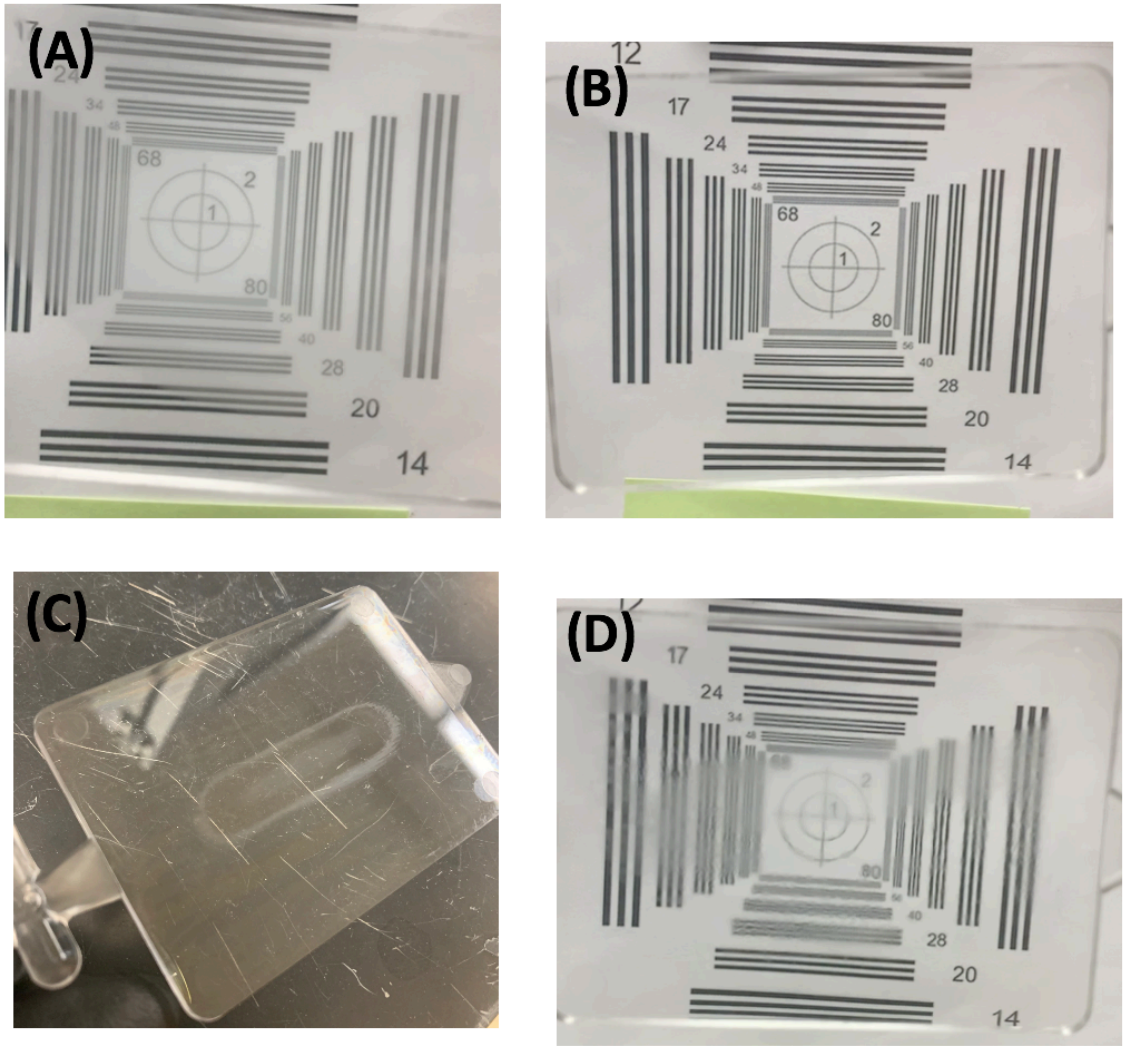

Figure 2.8 Photographs of (A) noncoated polycarbonate blank and (B) BPMPC coated polycarbonate sequentially after exposure to the fogging test, (C) immediately after the abrasion test, and (D) after post-abrasion fog test.

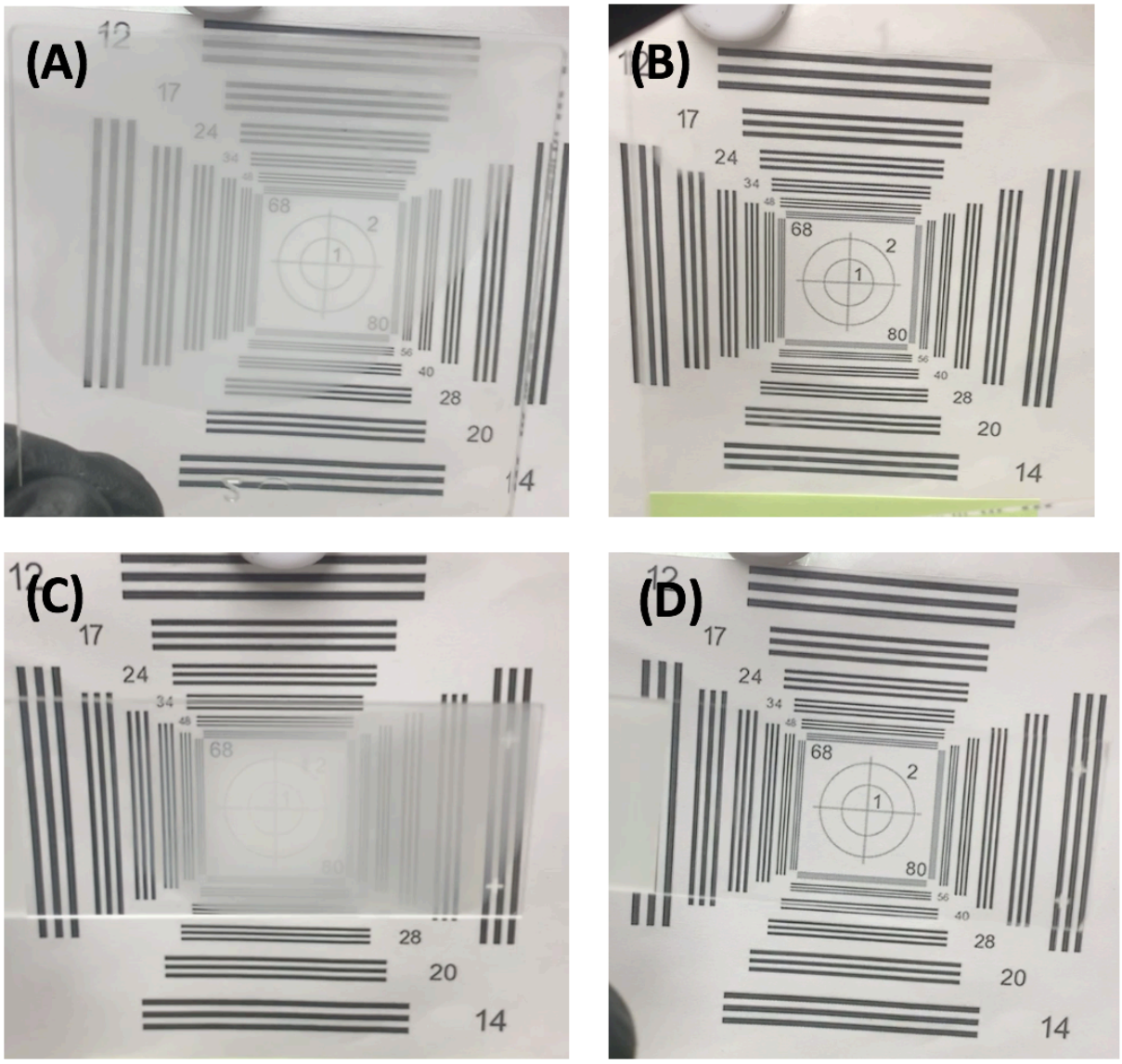

Figure 2.9 Photographs of (A) noncoated nylon blank and (C) iBTS modified glass slide immediately after fogging tests, and BPMPC coated (B) nylon and (D) iBTS modified glass slide after exposure to the abrasion and fogging tests.

3. Wavelength and Atmosphere Effects

In an effort to fully understand the characteristics of BPMPC crosslinking, UV-Vis spectroscopy was analyzed for kinetics of reaction. As shown in Figure 2.5 (254 nm air) a peak

is observed at approximately 350 nm that has not been previously identified for this BP copolymer. In addition, the moving isosbestic point at 300 nm indicates a clear side reaction occurring during irradiation. Kinetics of reaction are shown to be affected by atmospheric irradiation conditions. Investigation into these UV-Vis characterizations at different wavelengths and atmospheres will give a greater understanding of the overall BPMPC crosslinking process.

To characterize this reaction, 10 μL of 10 mg mL^{-1} BPMPC in ethanol solution was drop casted onto isobutyl trichlorosilane (iBTS) modified quartz substrates and solvent was allowed to evaporate. UV-Vis spectroscopy was used to investigate the crosslinking reaction, in which the increased irradiation time causes a decrease in BP carbonyl peak at 265 nm as hydrogen abstraction takes place. Figure 2.5 shows the UV-Vis spectra, where the maximum absorbance decreases after prolonged irradiation. In order to probe the crosslinking reaction, different irradiation conditions were analyzed. Atmospheric conditions are a likely source for oxidation to occur, therefore irradiation was done in both air (oxygenated) and inert (nitrogen) atmospheres. Additionally, the shifting isosbestic point and peak formations were observed to change between irradiation wavelengths, therefore irradiation at 254 and 365 nm was conducted.

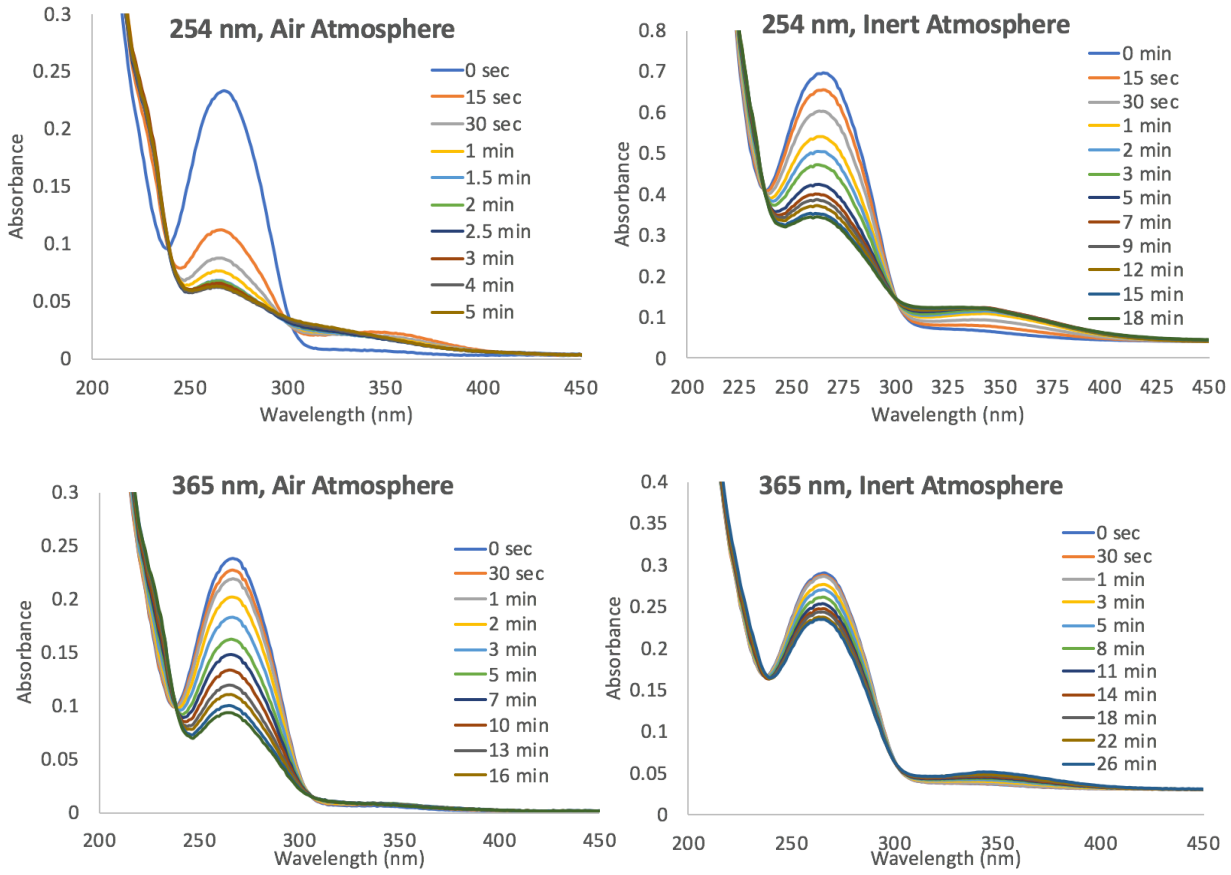

Figure 2.10 UV-Vis absorption spectrum of BPMPC, drop casted onto iBTS functionalized quartz substrate as a function of wavelength (254nm and 365 nm) and atmosphere (air and inert).

Previous research[23] has identified the 265 nm peak as the benzophenone carbonyl used to study reaction kinetics. However, there is a secondary peak at 350 nm that has not been characterized for BPMPC. First, the different electron arrangements in the molecular orbitals must be understood to identify the unknown peak at 350 nm in Figure 2.5. Upon irradiation of BPMPC, two possible excited singlet and triplet states can be achieved.[20] A π electron from the bonding orbital can be excited to the lowest-energy unoccupied orbital, π^*, making the $\pi - \pi^*$ transition (S_2). The nonbonded n electrons, found on the carbonyl oxygen, can also be excited to the π^* orbital, making what is known as the $n - \pi^*$ transition (S_1). Intersystem crossing (ISC)

then occurs from the singlet state (S_1) to triplet state (T_1 and T_2). This biradical triplet state then allows for hydrogen abstraction and crosslinking.

Irradiation of a broad spectrum of UV light occurs during UV-Vis spectroscopy, in which both $\pi - \pi^*$ and $n - \pi^*$ transitions for the BP carbonyl take place. The $n - \pi^*$ transition has lower energy relative to the $\pi - \pi^*$ transitions and occurs at higher wavelengths in UV-Vis spectroscopy than the higher energy excitation. Therefore, it can be concluded that the 350 nm peak seen in Figure 2.5 belongs to the $n - \pi^*$ transition, while the 265 nm peak represents the $\pi - \pi^*$ transition for excited BP carbonyl. Although the $n - \pi^*$ transition has lower relative energy, its absorption intensity is orders of magnitude less than the $\pi - \pi^*$ transition, due to the spatial proximity of the n and π electrons to the excited π^* state. In addition, the $n - \pi^*$ transition increases with increased irradiation, due to the change in planarity when hydrogen abstraction and crosslinking reactions occur.[35]

There are many conclusions that can be drawn through the comparison of different wavelengths (254 and 365 nm) and atmospheres (air and inert) for irradiation, specifically using UV-Vis spectroscopy to calculate kinetics of crosslinking from the decreasing carbonyl group's absorption. From previous research[22], kinetic constants for each reaction condition were calculated by normalizing initial peak maximum absorbance (265 nm) to 1 and describing further irradiation peak maxima by a single-exponential decay.

$$A_{normalized} = e^{-kt} + A_{\infty} \tag{2.1}$$

Where k is the reaction rate constant, t is time under UV-irradiation, and A_{∞} is the constant absorbance in infinite time. Table 2.2 shows the reaction constant, k, as calculated from the kinetics curves, exhibiting the significant decrease in the value of the rate constant between irradiation conditions of both wavelengths and atmospheres.

Using the carbonyl's absorption, the calculated rate of BP crosslinking are shown to be affected by both wavelength of irradiation, as well as atmospheric conditions. 254 nm irradiation in oxygenated air produces the fastest reaction kinetics that is an order of magnitude above all other reaction parameters (Figure 2.6). The 254 nm produces faster kinetics due to the increased energy of irradiation over 365 nm, allowing for a larger number of $\pi - \pi^*$ transitions. This higher probability of excitation is shown in Figure 2.5, by comparison of the $n - \pi^*$ peak intensities between 254 and 365 nm. The $n - \pi^*$ transition, as mentioned above, is less probable than the $\pi - \pi^*$ transition, and requires a greater amount of photon energy to occur. Therefore, because the 254 nm shows a larger $n - \pi^*$ peak than 365 nm, there will also be a corresponding increase in $\pi - \pi^*$ transitions or more crosslinking occurrences.

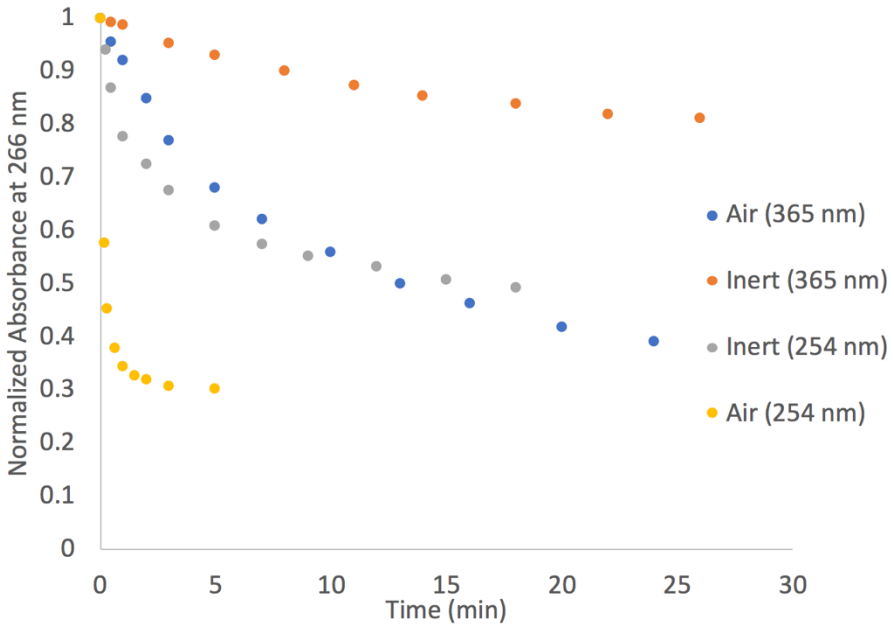

Figure 2.11 BPMPC photo-crosslinking kinetics study by UV-Vis spectroscopy.

Table 2.2 Characteristics of BPMPC crosslinked by different wavelengths and atmospheres.

sample	kinetics ($10^{-2}s^{-1}$)
254 nm, Air	8.93
254 nm, Inert	0.646
365 nm, Air	0.223
365 nm, Inert	0.131

It is hypothesized that the reduced rate constants from air to inert atmospheres is due to the formation of reactive oxygen species (ROS) in the oxygen rich atmosphere, that create a higher number of radicals in the zwitterionic copolymer system, allowing for total BP reactions to occur with higher frequency. ROS is a collective term for singlet oxygen, superoxide radicals, and any other oxidizing species formed subsequently.[29] ROS's play a critical role in photobleaching[27, 36-39] and oxidation.[40] Photobleaching is a potential cause for increased kinetics in oxygenated atmospheres. The kinetics calculation is based off of the BP carbonyl absorption, which represents the overall BP reactions, which includes oxidation. Therefore, the kinetics do not represent just the BP crosslinking, but rather any side reactions as well. This indicates that UV-Vis spectroscopy cannot be accurately used to exclusively show the extent of crosslinking.

Oxidation can clearly be seen in the isosbestic point (300 nm) movement and $n - \pi^*$ peak shape change in Figure 2.5 (254 nm air) that is not seen in other reaction conditions. This UV-Vis spectral movement indicates a side reaction, and due to the high energy and oxygenated atmosphere, oxidation of the BP moiety is likely occurring. This further validates the production of ROS species in that polymer system. Such spectral movements and peak changes are not seen in other reaction conditions, specifically 365 nm in oxygen rich air. In order to track the

oxidation, the isosbestic point between the $n - \pi^*$ and $\pi - \pi^*$ peaks, as well as $n - \pi^*$ peak shape, must be observed. However, as previously stated, the 365 nm wavelength does not provide enough energy to properly excite the $n - \pi^*$ transition, thus the isosbestic point and side peaks cannot be observed. Therefore, oxidation at 365 nm cannot be as accurately depicted using UV-Vis spectroscopy.

To further confirm the crosslinking reactions of the BPMPC in different conditions, FTIR was conducted on irradiated copolymers. In the IR spectra (Figure 2.7) the absorption peak at 1650 cm^{-1} has previously been assigned[23] as the C=O stretch of the BP ketone. Reduction of this peak would indicate the formation of a network polymer with covalent linkages as the BP undergoes hydrogen abstraction converting from a carbonyl to a hydroxide. Note, the spectrum is of the entire BPMPC copolymer, with a concentration of 2.4% BP, therefore the BP peak intensity is relatively proportional to other comonomers. Other notable peaks include 1240, 1080, and 970 cm^{-1} assigned to the PC groups. Surprisingly, despite the previously discussed rapid kinetics calculations for 254 nm irradiation in air over inert atmospheres, there is a significantly lower relative BP C=O peak for inert than air after irradiation at 254 nm. The lack of decrease due to BP crosslinking shown in air is very likely due to overlapping peak formation of the carbonyl groups formed during oxidation reactions.[28] In addition, there are relatively low BP C=O decreases for 365 nm as well, which may be attributed to the low intensity of irradiation, causing a lack of overall reactions occurring, as seen in the UV-Vis data. Lastly, it should be noted that these experiments were done without the purification step added into the synthesis. Unforeseen circumstances, such as Covid-19 laboratory shutdowns, prevented the continuation of experimentation to compare to purified BPMPC. Kinetics between BPMPC-RM

and BPMPC were evaluated to be nondifferentiable (section 1), however FTIR has not been studied.

Crosslinking could not be accurately measured by the reduction of the BP C=O IR intensity due to overlapping peak formation of carbonyls generated from oxidation. Accurately characterizing the extent of reaction and kinetics is vital for industrial application. Understanding the limitations of spectroscopy, as well as the polymer responses in different reaction conditions brings the ability for a successful anti-fog coating one step closer.

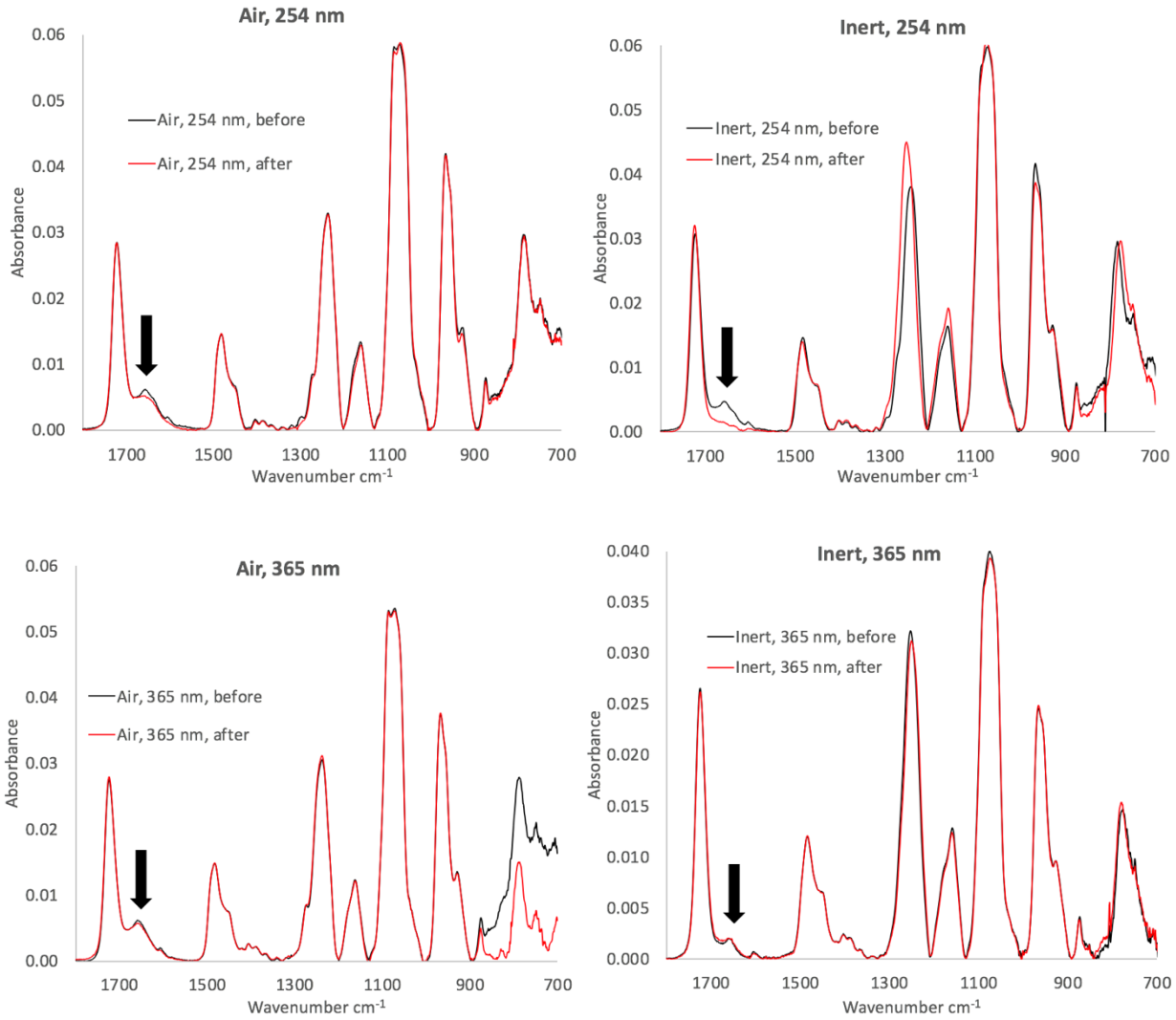

Figure 2.12 GATR-FTIR spectra of BPMPC coatings before and after 254 and 365 nm irradiation in air and inert atmospheres.

Conclusions

A zwitterionic copolymer, BPMPC, was shown to be a viable option for anti-fog, abrasion resistant functional coatings. An additional precipitation step was added to larger scale synthesis of BPMPC to minimize the detrimental effect of monomer impurity on abrasion resistance. BPMPC displayed substrate crosslinking affinity, due to the difference in rate of hydrogen abstraction on carbons with different radical stability. Substrates such as nylon, with rates of abstraction greater than the C-H bonds in the polymer itself, were shown to create robust crosslinking networks. Substrates that had slower abstraction rates, such as polycarbonate, did not create a coating that could withstand abrasion. Lastly, rates of kinetic reactions for BP were shown to be affected by wavelength of irradiation and atmospheric conditions. It was determined that UV-Vis and FTIR were not accurately characterizing the extent of BP crosslinking itself, due to photobleaching and oxidation. Overall, a greater understanding of the BPMPC polymer system was achieved and reinforced its ability to become a commercially viable option for functionalized anti-fog, abrasion-resistant coatings.

References

1. Dorman, G. P., G. D., Using Photolabile Ligands in Drug Discovery and Development. *Trends Biotechnol.* **2000,** *18*, 64−77.

2. Turgeon, A. J. H., B. A.; Bailey, R. C., Benzophenone-Based Photochemical Micropatterning of Biomolecules to Create Model Substrates and Instructive Biomaterials. *Method Cell Biol.* **2014,** *121*, 231-232.

3. Yang, P. Y., W. T., Surface Chemoselective Phototransformation of C-H Bonds on Organic Polymeric Materials and Related High-Tech Applications. *Chem Rev.* **2013,** *113* (7).

4. Cobley, A. J., Alternative Surface Modification Processes in Metal Finishing and Electronic Manufacturing Industries. *T I Met Finish* **2007,** *85* (6), 293-297.

5. Radu, A. S., S.; Byrne, R.; Slater, C.; Lau, K. T.; Diamond, D., Photonic Modulation of Surface Properties: A Novel Concept in Chemical Sensing. *J Phys D Appl Phys* **2007,** *40* (23), 7238-7244.

6. Zhao, J. M., A.; Ma. L.; Wang, X. J.; Ming, W. H., Terpolymer-based SIPN Coating with Exellent Anti-fogging and Frost-Resisting Properties. *RSC Adv.* **2015,** *5*, 102560-102566.

7. Chevallier, P. T., S.; Sarra-Bournet, C.; Turcotte, R.; Laroche, G., Characterization of Multilayer Anti-Fog Coatings. *2011* **2011,** *3*, 750-758.

8. Petit, J. B., E., General Frost Mechanism on Solid Substrates with Different Stiffness. *Langmuir* **2014,** *30*, 1160-1168.

9. Wang, Y. L., T. Q.; Li. S. H.; Sun, J. Q., Anti-fogging and Frost-resisting Polyelectrolyte Coatings Capable of Healing Scratches and Restoring Transparency. *Chem. Mater.* **2015,** *27*, 8058-8065.

10. Howarter, J. A. Y., J. P., Self-Cleaning and Next Generation Anti-Fog Surfaces and Coatings. *Macromol. Rapid Commun.* **2008,** *29*, 455-466.

11. Zhang, L. B. L., Y.; Sun, J. Q.; Shen, J. C., Mechanically Stable Antireflection and Anti-fogging Coatings Fabricated by The Layer-by-layer Deposition Process and Postcalcination. *Langmuir* **2008,** *24*, 10851-10857.

12. deLeon, A. A., R. C., Reversible Superhydrophilicity and Superhydrophobicity on a Lotus-Leaf Pattern. *ACS Appl Mater Inter* **2014,** *6*, 22666-22672.

13. Raza, A. D., B.; Zainab, G.; El-Newehy, M,; Al-Deyab, S. S.; Yu, J. Y. , Insitu Crosslinked Superwetting Nanofibrous Membranes for Ultrafast Oil-Water Seperation. *J. Mater. Chem. A* **2014,** *2*, 10137-10145.

14. Zhang, L. Z., N.; Xu, J., Fabrication and Application of Superhydrophilic Surfaces: A Review. *J. Adhes. Sci. Technol.* **2014,** *28*, 769-790.

15. Wang, R. H., K.; Fujishima, A.; Chikuni, M.; Kojima, E.; Kitamure, A.; Shimohigoshi, M.; Watanabe, T., Light-Induced Ampiphilic Surfaces. *Nature* **1997,** *338* (431-432).

16. Fujishima, A. Z., X. T.; Tryk, D. A., TiO2 Photocatalysis and Related Surface Phenomena. *Surf. Sci. Rep.* **2008,** *2008* (63), 515-582.

17. Lai, Y. K. T., Y. X.; Gong, J. J.; Gong, D. G.; Chi, L. F.; Lin, C. J.; Chen, Z., Transparent Superhydrophobic/Superhydrophilic TiO2-based Coatings for Self-Cleaning and Anti-fogging. *J. Mater. Chem.* **2012,** *22*, 7420-7426.

18. Gao, J. M., A.; Yatvin, J.; White, E.; Locklin, J., Permanently Grafted Icephobic Nanocomposites with High Abrasion Resistance. *J. Mater. Chem. A* **2016,** *4* (30), 11719-11728.

19. Liu, Q. L., J., Transparant Grafted Zwitterionic Copolymer Coatings That Exhibit Both Anti-fogging and Self-Cleaning Properties. *ACS Omega* **2018,** *3* (12), 17743-17750.

20. György Dorman, H. N., Abigail Pulsipher, and Glenn D. Prestwich, The Life of Pi Star: Exploring the Exciting and Forbidden Worlds of

the Benzophenone Photophore. *ACS, Chemical Reviews* **2016,** *116*, 15284−15398.

21. Crabtree, R. H., Introduction to Selective Functionalization of C-H bonds. *Chem Rev.* **2010,** *110* (2).

22. Liu, Q. L., J., Photocross-linking Kinetics Study of Benzophenone Containing Zwitterionic Copolymers. *ACS Omega* **2020**.

23. Liu, Q. S., P.; Handa, H.; Locklin, J., Covalent Grafting of Antifouling Phosphorylcholine-based Copolymers with Antimicrobial Nitric Oxide Releasing Polymers to Enhance Infection-Resistant Properties of Medical Device Coatings. *Langmuir* **2017,** *33* (45), 13105-13113.

24. Christensen, S., *Macromolecules* **2012,** *45*, 5237-5246.

25. Smets, G. J. E., S. N.; Oh, T. J., Photochemical Reactions on Polymers. *Pure Appl. Chem.* **1984,** *56*, 439-446.

26. Lin, A. A. S., V. R.; Tesoro, G.; Reiser, A.; Eachus R. , On the Crosslinking Mechanics of Benzophenone-containing Polyimides. *Macromolecules* **1988,** *21*, 1165-1169.

27. Brinkmann, T. S., D.; and Frimmel, F., Photobleaching of Humic Rich Dissolved Organic Matter. *Aquat. Sci.* **2003,** *65*, 415-424.

28. Lee, M. L., H.; Han, S.; Kim, H.; and Won, Y. , Photo-oxidation in the photobleaching process of non-linear optical polymer. *Thin Solid Films* **1996,** *283*, 247-250.

29. Zheng, Q. J., S.; Zhou, Z.; and Blanchard, S. , The Contribution of Reactive Oxygen Species to the Photobleaching of Organic Fluorophores. *Photochemistry and Photobiology* **2014,** *90*, 448-454.

30. Hou, A. F., G.; Zhuo, J.; Sun, G., UV Light-Induced Generation of Reactive Oxygen Species and Antimicrobial Properties of Cellulose Fabric Modified by 3,3',4,4'-Benzophenone Tetracarboxylic Acid. *ACS Appl. Mater. & Interfaces* **2015,** *7*, 27918-27924.

31. Yativin, J. G., J.; Locklin, J., Robust and Varied Attachment of Non-leaching Poly"-onium" Bactericidal Coatings to Reactive and Inert Surfaces. *CHem. Commun.* **2014,** *50*, 9433-9442.

32. Cohen, S. G. P., A.; Parsons, G. H., Photoreduction by Amines. *Chem Rev.* **1973,** *73*, 141-161.

33. Griller, D. H., J. A.; Marriott, P. R.; Scaiano, J. C, Absolute Rate Constants for the Reactions of tert-Butoxyl, teri-Butylperoxyl, and Benzophenone Triplet with Amines: The Importance of a Stereoelectronic Effect1. *J. Am. Chem. Soc.* **1981,** *103*, 619-623.

34. Giering, L. B., M.; Steel, C., Rate Studies of Aromatic Triplet Carbonyls with Hydrocarbons. *J. Am. Chem. Soc.* **1974,** *96*, 953-958.

35. Rau, H. a. L., E. , On the Rotation-Inversion Controversy on Photoisomerization of Azobenzenes. Experimental Proof of Inversion. *J. Am. Chem. Soc.* **1982,** *104* (6), 1616-1620.

36. Bonnett, R. a. M., G., Photobleaching of sensitisers used in photodynamic therapy. *Tetrahedron* **2001,** *57*, 9513-9547.

37. Chen, P. L., J.; Qian, Z.; Okasaki, T.; and Hayami, M., Study on the photooxidation of a near-infrared-absorbing benzothiazolone cyanine dye. *Dyes Pigm.* **1998,** *37*, 213-222.

38. Byers, G. G., S.; and Henrichs, P., Direct and Sensitized Photoxidation of Cyanine Dyes. *Photochem. Photobiol.* **1976,** *23*, 37-43.

39. Kuramoto, N. a. K., T., The contribution of singlet oxygen to the photofading of triphenylmethane and related dyes. . *Dyes Pigm.* **1982,** *3*, 49-58.

40. Lee, M. L., H.; Han, S.; Kim, H.; and Won, Y., Photo-oxidation in the photobleaching process of a non-linear optical polymer. *Thin Solid Films* **1996,** *283*, 247-250.

CHAPTER 3

CONCLUSIONS AND FUTURE OUTLOOK

Conclusions

Much consideration must be put into the process of upscaling a viable anti-fogging, abrasion resistant coating for the purpose of manufacturing high performance goggles. Synthesis of larger quantities of BPMPC, a zwitterionic copolymer, must remain facile and economical. However, purification steps were implemented to negate the detrimental effect of monomer impurity on abrasion resistance. This effect was due to the large amount of excess monomer crosslinking during irradiation, leading to a loosely connected network of polymers and attached monomers that could not withstand the normal wear and tear of daily eyewear use. The next consideration for manufacturing a goggle is the substrate and previous surface modifications. Abstraction of hydrogens by BP depends on the stability, location, and density of the hydrogens in the system. It was shown that if the BP had a higher abstraction rate with hydrogens on its own polymer chain than on the substrate, as was seen with polycarbonate, polymer-polymer crosslinking would be favored. In order for a robust network to be formed, the hydrogens in the substrate must be equal to or greater in rate of abstraction than the hydrogen in the BPMPC polymer. Nylon and iBTS modified glass formed an abrasion resistant polymer-substrate crosslinked network with BPMPC.

Lastly, rate of BP crosslinking was affected by wavelength of irradiation and atmospheric conditions. 254 nm displayed faster kinetics than 365 nm due to the increase in energy and

number of $\pi - \pi^*$ transitions. BPMPC displayed photobleaching and oxidation in the oxygenated atmosphere due to the increased number of ROS in the system. It was determined that UV-Vis and FTIR did not accurately portray the extent of crosslinking due to photobleaching and oxidation.

Future Work

Due to unforeseen circumstances, UV-Vis and FTIR analysis of purified BPMPC could not be conducted. Further experimentation on how the irradiation wavelength and atmosphere affect the crosslinking and reaction kinetics would be beneficial to the overall understanding of BPMPC chemistry. In addition, ellipsometry would be considered to determine extent of BP crosslinking, independent of side reactions, by calculation of gel fraction.

Optimization to a manufacturing line would be a logical next step, as large-scale synthesis could be optimized with the additional purification step. Experimentation to determine the effect of irradiation intensity kinetics, degradation, and anti-fogging properties would be completed. The correct substrate, or base coat, would need to be used, and optimization to commercial machinery would lead to a market ready anti-fog, abrasion-resistant coating for high-performance eyewear.

APPENDIX A

NMR SPECTRA OF COMPOUNDS

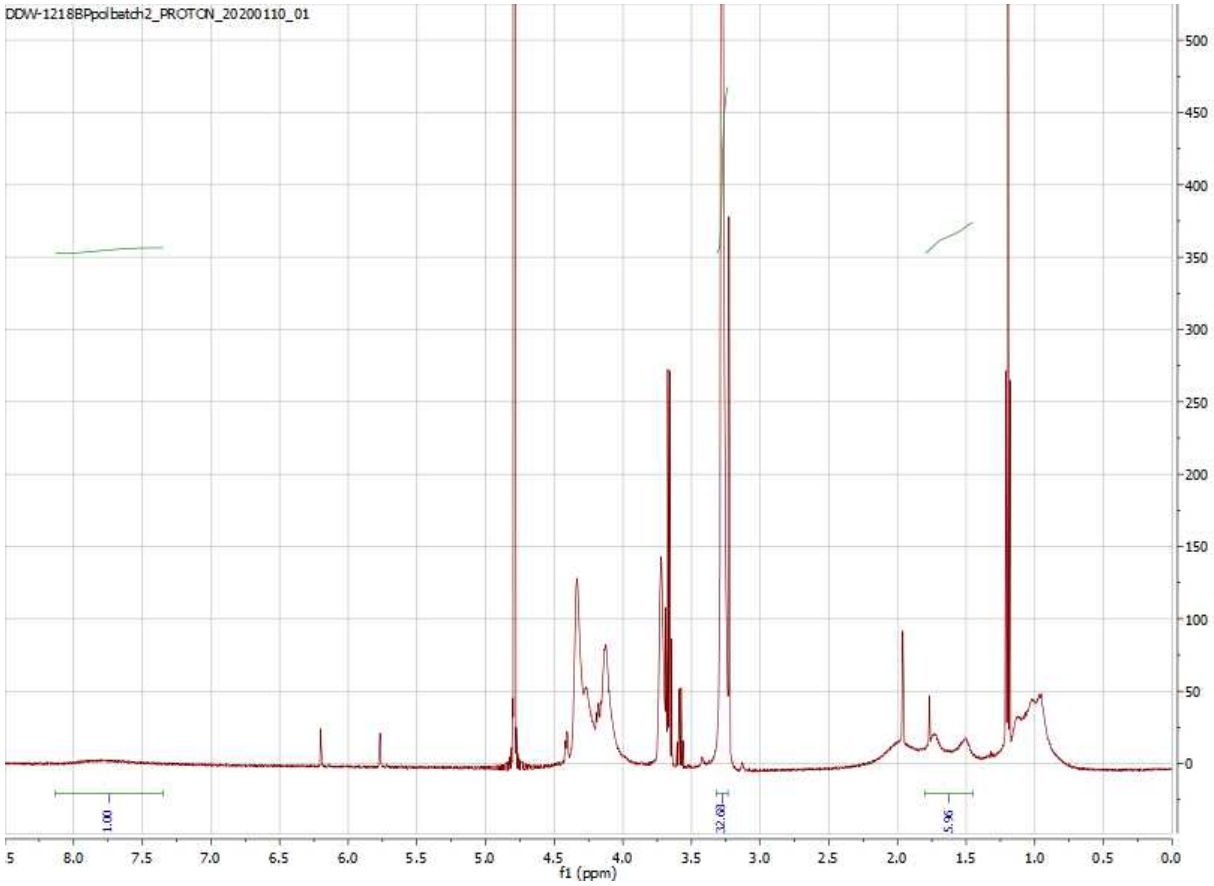

Figure A1 ^{1}H NMR of BPMPC-RM (batch 1/10/20).

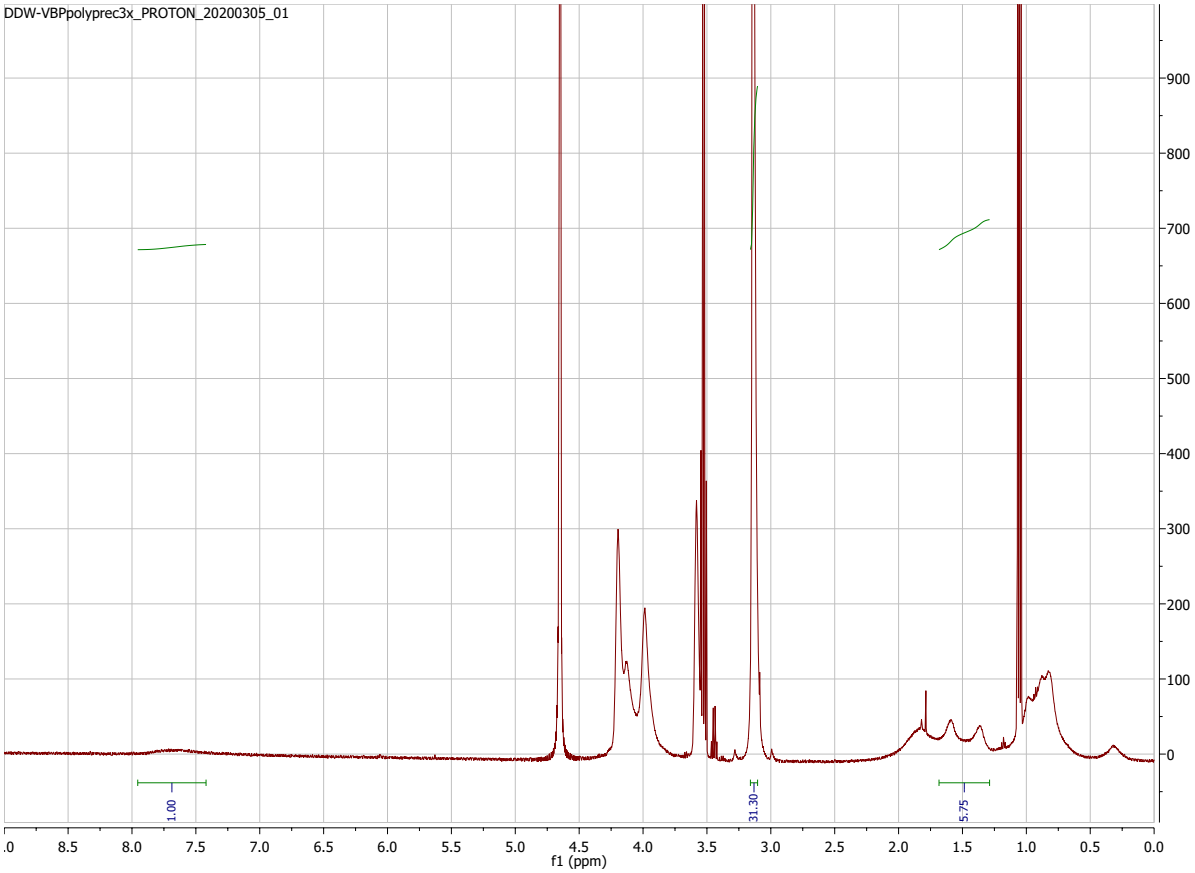

Figure A2 ^{1}H NMR of purified BPMPC (batch 1/10/20).

Table A1. Comonomer ratio's for BPMPC (batch 1/10/20).

Copolymer	BP%	MPC%	nBMA%	Observations
BPMPC-RM (batch 1/10/20)	2.1	69.4	28.5	Yellow, somewhat dissolve in EtOH
Purified BPMPC (batch 1/10/20)	2.4	70.0	27.8	White, dissolves in EtOH

APPENDIX B

KINETICS ANALYSIS

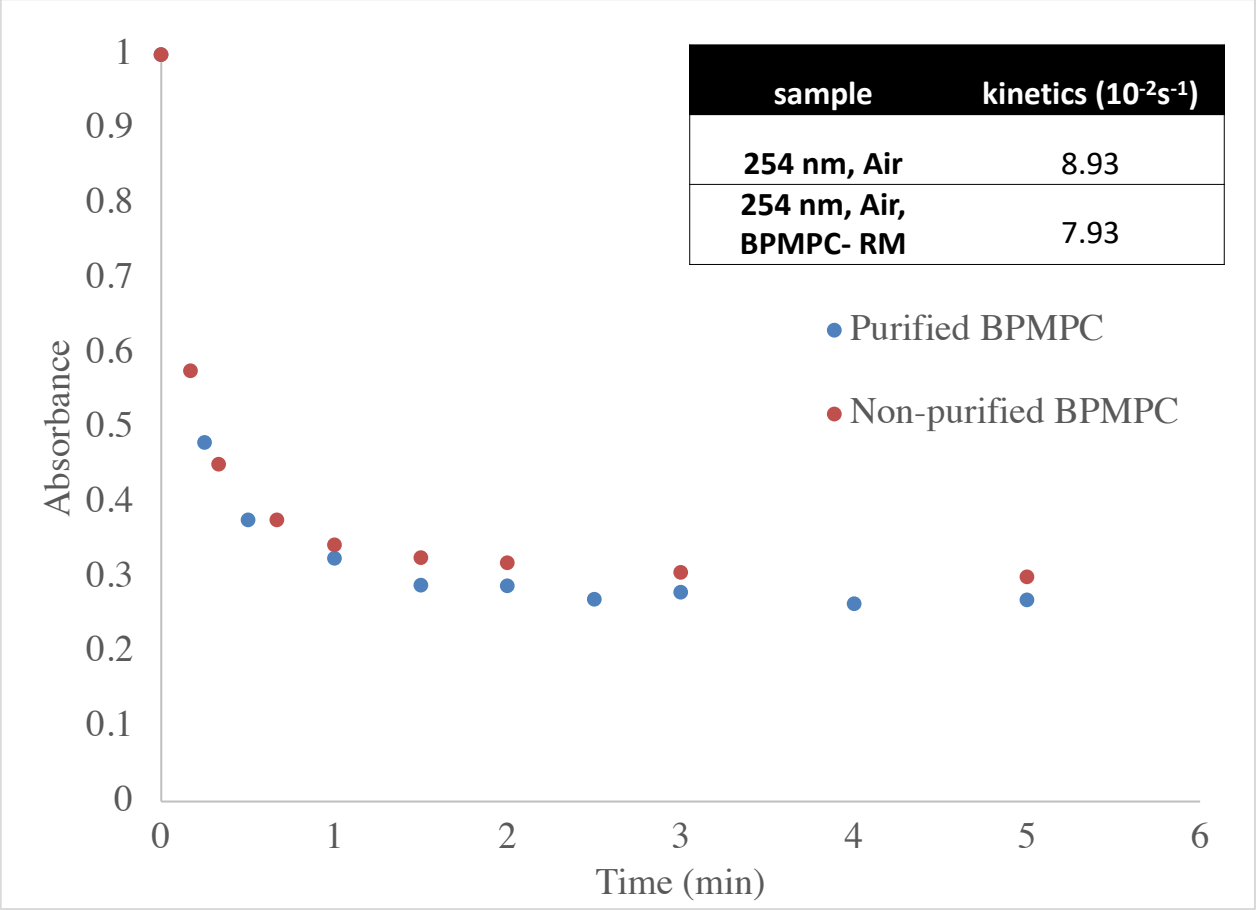

Figure B1 Kinetics comparison of BPMPC (purified) vs BPMPC-RM (residual monomer) at 254 nm irradiation.